

1 **Photochemical and Microbial Degradation of Chromophoric Dissolved Organic Matter**
2 **Exported from Tidal Marshes**

3 **Laura Logozzo^{1,†}, Maria Tzortziou¹, Patrick Neale², and Blake Clark³**

4 ¹The City College of New York, The City University of New York, Center of Discovery and Innovation,
5 85 St Nicholas Terrace, New York, NY 10031, USA. ²Smithsonian Environmental Research Center
6 (SERC), PO Box 28, Edgewater, MD 21037, USA. ³NASA Postdoctoral Program, NASA Goddard Space
7 Flight Center, 8800 Greenbelt Rd, Code 616.1, Greenbelt, MD 20771, USA.

8 [†] Current affiliation: School of the Environment, Yale University, 195 Prospect Street, New Haven, CT
9 06511, USA.

10 Corresponding Author: Maria Tzortziou (mtzortziou@ccny.cuny.edu)

11 **Key Points:**

12

- 13 Marsh dissolved organic matter export showed strong seasonal dependence, but seasonal
variability in its quality was significantly lower
- 14 Exposure to light increased the bioavailability of marsh-exported chromophoric dissolved organic
matter (CDOM)
- 15
- 16 Photobleaching decreased humic-like CDOM fluorescence, but increased microbial production of
humic-like CDOM fluorescence
- 17

18 **Abstract**

19 Wetlands export chromophoric dissolved organic matter (CDOM) to estuaries, where CDOM is removed
20 and transformed through biotic and abiotic process, subsequently impacting nutrient cycling, light
21 availability, ecosystem metabolism, and phytoplankton activity. We examined the bioavailability and
22 photoreactivity of CDOM exported from four Chesapeake Bay tidal marshes across three seasons and
23 along an estuarine salinity gradient using three incubation treatments: 14-day microbial (MD), 7-day
24 combined photochemical/microbial (PB+MD), and 7-day microbial incubation after photobleaching (MD
25 after PB). CDOM absorption at 300 nm (acDOM300) and dissolved organic carbon (DOC) concentrations
26 showed strong seasonality, with minima in winter, but CDOM quality (absorption spectral slopes,
27 fluorescence component ratios) was less variable seasonally. PB+MD over 7 days decreased acDOM300 (−
28 56.0%), humic-like fluorescence (−67.6%), and DOC (−17.8%), but increased the spectral slope ratio S_R
29 ($=S_{275-295}/S_{300-350}$) (+94.8%), suggesting a decrease in CDOM molecular weight. Photochemistry
30 dominated the PB+MD treatment. Photoreactivity was greater during the winter and in marsh/watershed
31 versus down-estuary sites, likely due to less previous light exposure. Prior photobleaching increased the
32 bioavailability of marsh-exported CDOM, resulting in a greater loss of acDOM300 and DOC, and a greater
33 increase in humic-like fluorescence (−6.0%, −5.9%, and +18.4% change, respectively, over 7-day MD
34 after PB incubations, versus −2.8%, −5.5%, and +2.6% change, respectively, over 14-day MD
35 incubations). CDOM exported from a marsh downstream of a major wastewater treatment plant showed
36 the greatest photoreactivity and bioavailability. This highlights the significance of human activity on
37 estuarine CDOM quality and biogeochemical cycles.

38 **Plain Language Summary**

39 Marshes are sources of colored dissolved organic matter (CDOM) to estuaries, where CDOM can be
40 transformed or removed by ultraviolet (UV) radiation or microbes. We examined CDOM susceptibility to
41 UV radiation and microbial degradation from four Chesapeake Bay marshes and along a down-estuary
42 salinity gradient, using incubation experiments with samples collected in the summer, fall, and winter.
43 Our results showed that although more CDOM is exported by marshes in the summer, the quality of this
44 material (based on optical proxies for CDOM composition) was consistent seasonally and interannually.
45 Microbial processing removed a small, but significant, amount of CDOM and increased the contribution
46 of humic-like CDOM typically associated with terrestrial sources. Microbial degradation combined with
47 UV exposure decreased the amount of CDOM and the contribution of humic-like CDOM. Microbial
48 degradation after exposure to UV light resulted in a greater loss of DOC and more production of humic-
49 like CDOM compared to microbial degradation alone, suggesting exposure to light enhances the microbial
50 utilization of marsh-exported CDOM. A marsh downstream of a major wastewater treatment plant
51 exported CDOM that was more susceptible to UV and microbial degradation, suggesting that human
52 activity can have significant effects on estuarine biogeochemical cycles, water quality, and ecosystem
53 productivity.

54 **1 Introduction**

55 Dissolved organic matter (DOM) is one of the most important biogeochemical components influencing
56 productivity, nutrient cycling, and optical properties of aquatic environments. DOM fuels heterotrophic
57 production in inland and coastal waters by providing carbon and nitrogen (Fellman et al., 2008), it limits
58 the amount of UV-radiation and visible light in the ocean (Bricaud et al., 1981), and it makes up one of
59 the largest reservoirs of carbon, with marine DOM storing as much carbon as that in atmospheric CO₂
60 (Hansell et al., 2009). DOM is the soluble portion of organic matter, operationally defined as organic

61 molecules that pass through a 0.2 μm filter (Putter, 1907). It is primarily composed of dissolved organic
62 carbon (DOC), in addition to dissolved organic nitrogen (DON), dissolved organic phosphorous (DOP),
63 and dissolved organic sulfur (DOS), thus contributing to the nutrient pool in aquatic environments. The
64 optically active fraction of DOM that absorbs light selectively is known as chromophoric dissolved
65 organic matter (CDOM) and a portion of the CDOM pool also fluoresces.

66 In coastal waters, CDOM is a complex mixture of allochthonous plant or soil derived compounds exported
67 by rivers and wetlands and autochthonous sources derived from phytoplankton and detritus (Hedges,
68 1992; Maie et al., 2007; Qualls et al., 1991; Rochelle-Newall & Fisher, 2002; Tzortziou et al., 2008).
69 Rivers and estuaries export $0.2 \pm 0.05 \text{ Pg}$ of DOC annually (Dai et al., 2012; Meybeck, 1982; Seitzinger
70 et al., 2005), making these systems along the terrestrial-aquatic interface important sources of DOM to
71 marine ecosystems. However, only a relatively small portion of terrigenous DOM makes up the oceanic
72 DOM pool (Hedges, 1992), indicating rapid loss and transformation by flocculation and microbial and
73 photochemical degradation processes in estuaries.

74 A particularly important source of terrestrial DOM to coastal ecosystems is tidal wetlands (Jordan et al.,
75 1983, 1991a; Nixon, 1980; Tzortziou et al., 2008, 2011; Wetzel, 1992), which export large quantities of
76 CDOM that is optically distinct from the surrounding aquatic system (Thurman, 1985; Tzortziou et al.,
77 2008). As a result, wetland CDOM has numerous impacts on the biogeochemistry, optical properties, and
78 biology of coastal waters, and often provides the carbon inputs necessary to sustain the net heterotrophy
79 of estuarine ecosystems (Schlesinger & Bernhardt, 2013). Recent studies suggest that the lateral flux of
80 total carbon from tidal wetlands to estuaries is $16 \pm 10 \text{ Tg C}$ per year for North America, but these
81 estimates are characterized by particularly high uncertainty (Windham-Myers et al., 2018). Net export of
82 dissolved carbon is poorly constrained by observations in these ecosystems, and, thus, wetland
83 contributions of CDOM and DOC to adjacent waters are often not included in coastal ocean photochemical
84 and biogeochemical models (Ward et al., 2020; Windham-Myers et al., 2018).

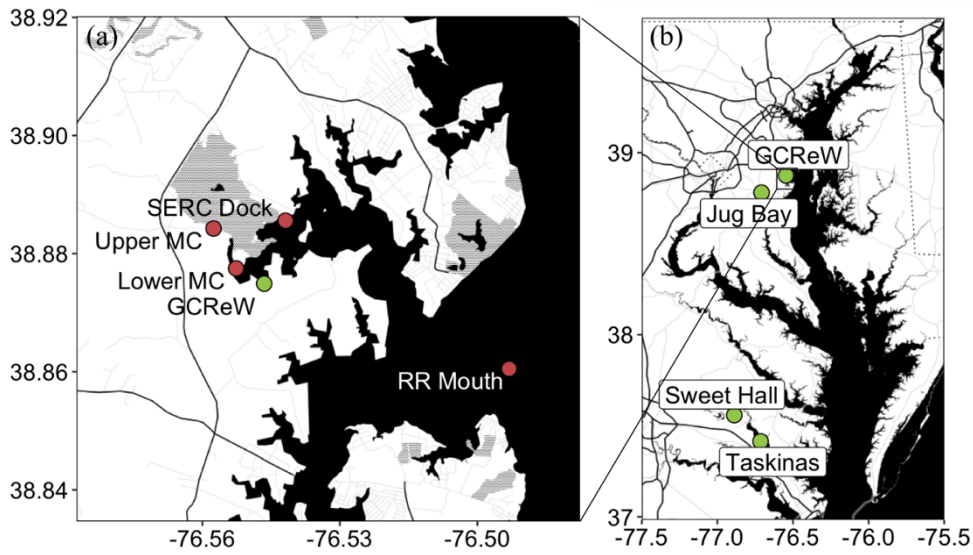
85 Wetland-exported CDOM tends to be mainly humic-like (i.e., made up of compounds such as lignin,
86 tannins, and polyphenols with high molecular weight and high aromaticity), and therefore, more strongly
87 light absorbing (C. D. Clark et al., 2008; Tzortziou et al., 2008; Wagner et al., 2015). While photochemical
88 degradation of terrestrial CDOM has been shown to lead to an increase in its lability (Moran et al., 1999;
89 Tranvik et al., 1999), its influence on the bioavailability of marsh-exported CDOM specifically has not
90 been as widely studied. Recent studies acknowledge the contribution of labile CDOM from bogs and
91 forested wetlands (Fellman et al., 2008), but the relative importance of environmental factors and source
92 material is largely unknown. The photoreactivity and bioavailability (two factors that make up CDOM
93 quality) of marsh-exported CDOM and how these vary seasonally, inter-annually, and across marsh
94 systems is not well characterized. This limits representation of these key processes in ecosystem models
95 and increases uncertainty in predictions of the fate of this carbon pool in the coastal ocean. As a result, an
96 essential piece in understanding the dynamics and functioning of temperate estuaries is missing, making
97 it difficult to predict the impacts of climate and coastal land-use changes on coastal biogeochemical
98 cycling and estuarine productivity.

99 We conducted a series of incubation experiments to characterize the quantity and quality of DOM exported
100 from four tidal marsh systems in the Chesapeake Bay and associated tidal rivers, characterized by different
101 vegetation properties, water quality, and salinity regimes. The bioavailability and photoreactivity was
102 measured for DOM exported from these marsh systems (GCReW, Jug Bay, Taskinas, and Sweet Hall)
103 and along a salinity gradient in the Rhode River sub-estuary. For each set of incubations, the influence of
104 photochemical transformations on the bioavailability of DOM was also assessed. Incubations were

105 performed under the same experimental conditions (i.e., temperature, light exposure) for DOM samples
 106 collected in the summer, fall, and winter to characterize seasonal and source-related differences in DOM
 107 microbial and photochemical degradability. Measurements across freshwater, brackish and heavily human-
 108 influenced marsh systems provide new insights into the role of marsh DOM outwelling in estuarine
 109 photochemical processes, biogeochemical cycles, and microbial ecology. The marshes and sub-estuary
 110 analyzed in this study have characteristics typical of temperate marshes and sub-estuaries, and as such,
 111 may be representative of many coastal systems in other temperate regions.

112 2 Methods

113 2.1 Research sites



114

115 **Figure 1.** (a) Sampling sites on the Rhode River sub-estuary, and (b) marsh sampling sites on Chesapeake
 116 Bay. Marsh sites are denoted in green. Map tiles by Stamen Design, under CC BY 3.0. Data by
 117 OpenStreetMap, under ODbL. Plotted using ggmap (Kahle & Wickham, 2013).

118 To quantify the lability and photoreactivity of estuarine and marsh-exported DOM across different
 119 systems and seasons, incubation experiments were performed on samples collected from tidal creeks
 120 draining freshwater and brackish marshes in Chesapeake Bay over the summer and fall of 2016, the winter
 121 of 2016-2017, and along a salinity gradient on the Rhode River sub-estuary in the summer of 2016 (Figure
 122 1; Table 1). The Kirkpatrick Marsh, also known as the Global Change Research Wetland (GCReW), is a
 123 high-elevation, brackish tidal marsh located on the Rhode River sub-estuary and is the main wetland
 124 source of DOM to the Rhode River (J. B. Clark et al., 2020; Jordan et al., 1983; Tzortziou et al., 2008,
 125 2011). It is located near the Smithsonian Environmental Research Center (SERC) and is dominated by
 126 *Spartina patens*, *Spartina cynosuroides*, *Distichlis spicata*, *Iva frutescens*, and *Scirpus olneyi* (Jordan et
 127 al., 1983). Taskinas is a brackish tidal marsh located on the York River and is dominated by *Spartina*
 128 *patens* and *Distichlis spicata* (Perry & Atkinson, 1997). Jug Bay and Sweet Hall are freshwater marshes.
 129 Jug Bay is located on the Patuxent River and is highly influenced by urban and suburban development
 130 (Swarth et al., 2013); it is also located directly down-stream (< 4 km) of a major wastewater treatment
 131 plant (WWTP), with a capacity of 30 million gallons per day, that has been reported to contribute 29% of
 132 the N-load and 48% of the P load of all WWTPs to the Patuxent River (Karth et al., 2013). While the
 133 WWTP began implementing enhanced nutrient removal (ENR) techniques in 2011 and nutrient

134 concentrations in the river decreased, phosphates remained relatively high, particularly in the summer and
 135 fall, indicating that the WWTP continues to contribute to nutrient concentrations despite ENR
 136 implementation. The Jug Bay system has a mix of persistent and primarily non-persistent emergent
 137 vegetation, including *Leersia oryzoides*, *Hibiscus moscheutos*, *Peltandra virginica*, *Phragmites australis*,
 138 *Polygonum arifolium*, and *Typha × glauca* (high marsh) and *Nuphar lutea*, *Pontederia cordata*, and
 139 *Zizania aquatica* (low marsh) (Swarth et al., 2013). Sampling was conducted near the low marsh portion
 140 of Jug Bay, making the vegetation characteristics at the sampling site distinct from the other marshes.
 141 Sweet Hall is located on the York River and is dominated by *Peltandra virginica*, *Carex stricta*, *Leersia*
 142 *oryzoides*, *Polygonum punctatum*, and *Polygonum arifolium* (Perry & Atkinson, 1997).

143 In addition to sampling at GCReW, we also sampled a number of sites along a down-estuary salinity
 144 gradient along the Rhode River at low tide: Upper Muddy Creek (Upper MC), Lower Muddy Creek
 145 (Lower MC), the SERC Dock and the Rhode River Mouth (RR Mouth) (Figure 1; Table 1). Upper Muddy
 146 Creek is located in an upstream reach of Muddy Creek (the main source of freshwater to the Rhode River),
 147 and is surrounded mostly by forest and mud flats, and thus CDOM from this site can be considered “non-
 148 marsh terrestrial” or watershed CDOM (Tzortziou et al., 2011). Lower Muddy Creek is located at the
 149 intersection of Muddy Creek and the Rhode River, and therefore, waters there receive a mixture of
 150 watershed and “estuarine” CDOM. The influence of GCReW may also be significant at Lower Muddy
 151 Creek. Water at the SERC Dock contains a mixture of marsh and estuarine CDOM, but with less marsh
 152 influence than waters closer to GCReW (Tzortziou et al., 2011). Lastly, the Rhode River Mouth is where
 153 the confluence of the Rhode and West Rivers opens to the main stem of Chesapeake Bay; it is therefore
 154 the most down-estuary endmember of all the sites (Tzortziou et al., 2008, 2011). Tzortziou et al. (2011)
 155 showed that along a gradient from GCReW to the Rhode River mouth at low tide, mixing was
 156 nonconservative for DOC and CDOM absorption and fluorescence, suggestive of DOC and CDOM
 157 degradation and/or transformation by photochemistry in particular (J. B. Clark et al., 2020). Therefore,
 158 sites along this gradient at low tide are representative of differences in DOC and CDOM quality both due
 159 to dilution with estuarine water and prior photochemical transformation during transport.

Incubation ID	Sampling Site(s)	Latitude/Longitude	Date of Sampling	Incubation Start
16-6	Upper MC	38.8843, -76.5576	6/28/16	6/28/16
	RR Mouth	38.8605, -76.4931	6/28/16	
16-6	Lower MC	38.8775, -76.5527	6/29/16	6/29/16
16-7	Jug Bay	38.7807, -76.7081	7/20/16	7/20/16
	Taskinas	37.4150, -76.7144	7/18/16	
16-7	GCReW	38.8749, -76.5465	7/21/16	7/21/16
	SERC Dock	38.8856, -76.5419	7/21/16	
16-8	GCReW	38.8749, -76.5465	10/19/2016	10/20/16
	Sweet Hall	37.5589, -76.8883	10/18/2016	
16-8	Taskinas	37.4150, -76.7144	10/18/2016	10/21/16
	Jug Bay	38.7807, -76.7081	10/19/2016	
17-1	GCReW	38.8749, -76.5465	1/5/2016	1/7/16
	Jug Bay	38.7807, -76.7081	1/5/2016	

17-1	Taskinas	37.4150, -76.7144	1/5/2016	1/8/16
	Sweet Hall	37.5589, -76.8883	1/5/2016	

160 **Table 1.** *Dates and Sampling Sites for Incubation Experiments Performed from June 2016 to January*
 161 *2017.*

162 **2.2 Sample collection and filtering**

163 Water samples were collected at each site within a time-window of ± 30 minutes from low tide, stored in
 164 the dark at 4°C , and in almost all cases filtered immediately upon collection (< 1 day storage) for 2-week
 165 dark and light incubation experiments. For marsh-exported CDOM, water samples were collected at tidal
 166 creeks draining each marsh ± 30 minutes from low tide, when the influence of marsh outwelling on
 167 adjacent estuarine water properties is the strongest (C. D. Clark et al., 2008; Jordan et al., 1983; Tzortziu
 168 et al., 2008).

169 We used glass-fiber filters (GF/F, nominal pore size of $0.7\text{ }\mu\text{m}$) to remove particulate material, but to
 170 retain some bacteria in the filtrate. It is important to note that only a portion (35-43%, according to Lee et
 171 al., 1995) of the total bacterial cell count passes through a GF/F and that the filter preferentially removes
 172 larger cells (i.e., diameters greater than $0.7\text{ }\mu\text{m}$). 100 mL of the filtrate was distributed either into
 173 combusted 120 mL amber bottles (dark treatments) or acid-soaked Teflon (Nalgene FEP) bottles (light
 174 treatments) (Text S1, Figure S1).

175 A portion of the GF/F filtrate was also subsequently filtered through a $0.2\text{ }\mu\text{m}$ filter (Nuclepore) and kept
 176 in the dark for 14 days as a presumed “control” treatment, or exposed to 7 days of light as presumed
 177 “photobleaching only” treatment. Although most studies have assumed samples filtered through a $0.2\text{ }\mu\text{m}$
 178 filter contain no bacteria (Lu et al., 2013; Stedmon & Markager, 2005; Zhang et al., 2013), we report here
 179 data on microbial cell counts showing that in our systems, enough inoculum passes through $0.2\text{ }\mu\text{m}$ filters
 180 to result in significant microbial growth in these fractions (see Results). Similar results were previously
 181 reported across a variety of ecosystems (Brailsford et al., 2017; Elhadidy et al., 2016; Liu et al., 2019;
 182 Obayashi & Suzuki, 2019; Wang et al., 2008). Other results from these treatments (e.g., photoreactivity
 183 estimates) are not presented since the presence of bacteria confounds their interpretation as “control” or
 184 “photobleaching only”.

185 **2.3 Incubations**

186 There were three treatments for the incubations: 14-day dark incubation (to assess microbial-only
 187 degradation, “MD”), 7-day light incubation (combined photochemical and microbial degradation “PB +
 188 MD”), and a 7 day dark incubation following the 7-day light incubation (to examine effects of previous
 189 light exposure on microbial degradation, “MD after PB”). The lengths of the incubations were chosen
 190 based on a typical residence time of a conservative tracer in the Rhode River from head of tide to the
 191 mouth of the sub-estuary, which is about 7 days under low flow conditions (Jordan et al., 1991b). All three
 192 treatments were incubated at 24°C (details in Text S2), in order to remove temperature as a potential
 193 confounding variable impacting DOM bioavailability and photoreactivity. The incubation temperature
 194 was chosen as 24°C since this is close to the average summer surface water temperature on the Rhode
 195 River. Incubations were started within 1-2 days of sample filtration; treatments were kept in the dark at
 196 4°C until the start of the incubations. Four replicate bottles were used for the microbial-only treatment
 197 (14-day incubation) and three each for the combined photochemical and microbial (7-day incubation) and
 198 microbial after photobleaching (7-day incubation) treatments; only three replicate bottles were used for

199 the light incubations due to space limitations in the UV-exposure set-up. The microbial-only treatment
200 remained in the dark over the course of the 14-day incubation and the bottles were inverted once per day
201 to reduce settling and aggregation. For the combined photochemical and microbial treatment, a UV-
202 transmitting acrylic Plexiglas sheet was placed approximately one inch above two Q-labs UVA340 lamps.
203 The Teflon bottles with 100 mL of the sample filtrate were placed on top of the UV-transmitting acrylic
204 sheet ("Plexiglas"), in two rows above the lamps with the center of the bottles centered on each lamp tube
205 (Figure S2-S3). The 100 mL of filtrate filled the Teflon bottles to a depth of about 4 cm. These bottles
206 were also inverted once per day to reduce settling, and their positions above the lamp were displaced each
207 day so that all bottles received approximately the same exposure over the course of the incubation.

208 UV spectral irradiance (284-650 nm) was measured at the upper surface of the Plexiglas at each bottle
209 position using a fiber optic spectroradiometer as described by Neale and Fritz (2001). While UVA340
210 lamps mainly emit in the UV (Figure S4), there is also a minor emission in the PAR (400-700 nm) mostly
211 from emission lines at 436 and 546 nm. Scalar (4π) measurements of this PAR emission (on the order of
212 $10 \mu\text{mol m}^{-2} \text{s}^{-1}$) were made at each bottle position both at the upper surface of the Plexiglas (dry) and at
213 mid-depth in the incubation bottles with 100 mL of deionized water using a QSL 2100 probe (Biospherical
214 Instruments). The in-bottle/upper-surface ratio of PAR together with the spectral transmission of the
215 Teflon bottles (relative to PAR, Figure S1) was applied to the upper-surface-measured UV spectrum to
216 estimate within-bottle UV exposure. This adjustment accounted for the optical effects of refraction,
217 scattering and spectral filtering by Teflon on within bottle exposure. Average exposure to total UV
218 irradiance (after accounting for filtrate self-shading, see Text S3) was 15.16 W m^{-2} (Table S1); absorbed
219 UV exposure over 24 h was about the same as the UV-exposure over a cloud-free summer day (June 21)
220 in the Rhode River surface water, based on the average CDOM absorption spectrum of each sample (see
221 Text S3, Table S1 and Figure S4). While small phototrophic picoplankton may be present in GF/F filtrate,
222 there was no evidence of any photosynthetic pigment absorbance in the spectral scans. For the effects of
223 photobleaching on microbial ("MD after PB") treatment, GF/F-filtered water samples that were exposed
224 to light for 1 week were placed in the dark for the second week to quantify the impacts of CDOM
225 photochemical degradation on its microbial availability.

226 2.4 Microbial Cell Counts

227 At selected time points in the incubations of October 2016 and January 2017, a 1.8 mL aliquot was taken
228 from each replicate incubation container (dark and light), fixed with 180 μL of 20% paraformaldehyde,
229 flash frozen at -80°C , and stored until processed (within a week). For analysis, the samples were thawed
230 and then stained with SYBR Green nucleic acid stain, incubating for at least 30 mins. Cell count based
231 on SYBR green fluorescence was performed with a BD C6 Accuri flow cytometer at the University of
232 Maryland Center for Environmental Horn Point Laboratory Cell Analysis Center. Before each sample
233 processing, the flow cytometer was validated with factory supplied 6- and 8- fluorescence peak beads
234 according to the BD Accuri software guide standards
235 (https://www.bdbiosciences.com/documents/BD_Accuri_CSampler_Software_User_Guide.pdf).

236 2.5 Measurements and PARAFAC modeling

237 Measurements were taken at three time points during the incubation: day 0, day 7, and day 14 (Text S4).
238 Samples were stored in a refrigerator at 4°C until measurement, which occurred within two days of the
239 incubation time point. The exception was October 2016, when travel to and from SERC prevented
240 immediate measurement; absorption and fluorescence measurements for this incubation were conducted
241 within 2 weeks of the incubation time point. DOC concentrations were measured within three months of

242 the incubation time point. All samples were stored in a refrigerator at 4°C between the incubation time
 243 point and the time of measurement; DOC samples were not acidified prior to analysis.

244 DOC concentrations were measured on a Shimadzu TOC-V CSH Total Organic Carbon analyzer using
 245 high temperature combustion. Determinations followed the manufacturer's recommended protocol for
 246 non-purgeable organic carbon based on calibration with potassium hydrogen phthalate.

247 CDOM absorption spectra ($a_{CDOM}[\lambda]$) were measured using a CARY-IV dual-beam spectrophotometer
 248 and 1 cm path-length, acid-washed and deionized water (DI)-rinsed, quartz cuvettes. Measurements (270-
 249 750 nm spectral range and at 2-nm resolution) were baseline corrected using DI, with a blank run at the
 250 beginning and end of the run, and every 5 samples. Duplicate measurements were performed on each
 251 sample. $a_{CDOM}(\lambda)$ was calculated from the optical density (OD) and path length (l_g , which for our
 252 measurements was 1 cm = 0.01 m):

$$253 \quad a_{CDOM}(\lambda) = 2.303 \frac{OD(\lambda)}{l_g}$$

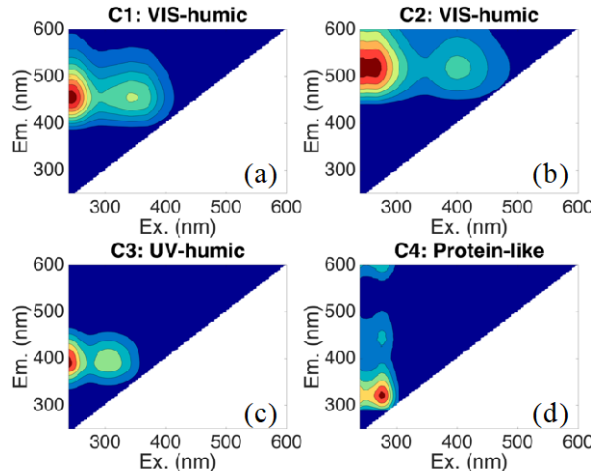
254 Consistent with other studies (C. D. Clark et al., 2008; Helms et al., 2008; Osburn & Stedmon, 2011),
 255 changes in CDOM absorption magnitude are reported at 300 nm ($a_{CDOM}300$). To examine changes in
 256 CDOM absorption spectral characteristics, we estimated the CDOM absorption slopes in the 275-295 nm
 257 spectral region ($S_{275-295}$) and the 350-400 nm spectral region ($S_{350-400}$) following Helms et al., (2008), by
 258 fitting a linear regression to the log-transformed $a_{CDOM}(\lambda)$ for each wavelength range (275-295 nm and
 259 350-400 nm). Changes in the slope ratio S_R , defined as $S_R = S_{275-295}/S_{350-400}$, are also shown, as S_R was
 260 previously reported to be a good indicator of DOM molecular weight (MW) and photochemically induced
 261 shifts in MW across water types (Helms et al., 2008).

262 Fluorescence excitation-emission matrices (EEMs) were measured using a SPEX Fluoromax-3
 263 spectrofluorometer. EEMs were measured for excitation wavelengths 240 to 600 nm (5 nm resolution) at
 264 emission wavelengths 250 to 600 nm (2 nm resolution). Fluorescence was corrected for absorption within
 265 the sample (inner-filter effect) using the absorption spectra measured spectrophotometrically following
 266 Kothawala et al. (2013). A DI EEM was measured for each set of sample EEMs run; after the inner-filter
 267 corrections, the DI EEM was subtracted from the sample EEM and then converted to Raman Units, using
 268 the area under the Raman scattering peak (excitation: 250 nm and emission: 370 to 428 nm).

269 EEMs were analyzed using parallel factor (PARAFAC) analysis, a multivariate modeling technique that
 270 decomposes the CDOM fluorescence signature into individual fluorescence components (Stedmon & Bro,
 271 2008). We compared the four PARAFAC components output from our model (Figure 2) to the OpenFluor
 272 database (Murphy et al., 2014). Descriptions of each component and references to similar components are
 273 described in detail in Table 2. The C1 fluorescence component (VIS-humic-like) was similar to terrestrial
 274 humic-like components from OpenFluor, and has been shown to be well-correlated with dissolved lignin
 275 concentration (Osburn, Boyd, et al., 2016). C2 (VIS-humic-like) was similar to spectra from soil fulvic
 276 acids and spectra from soil leachate (Osburn, Handsel, et al., 2016), and thus is described as terrestrial
 277 humic-like or soil fulvic-like fluorescence. C3 (UV-humic-like or marine-humic-like), is generally
 278 ubiquitous, and commonly present in estuarine and marine water, but also wastewater. It is often thought
 279 of as microbially-produced (Coble, 1996). C4 was similar to the fluorescence spectra of aromatic amino-
 280 acids (Bianchi et al., 2014; Osburn, Boyd, et al., 2016), and thus is described as protein-like.

281 The percent change for each parameter over each incubation was estimated as the difference between the
 282 measurement at the end of the incubation (either day 7 or day 14) and initial (day 0) values, divided by
 283 the initial value and multiplied by 100%. The impacts of light exposure on microbial availability were

284 determined by comparing the day 14 measurements to the day 7 measurements, where day 7 is the “initial”
 285 (i.e., the starting point for microbial degradation after 7 days of light exposure).



286

287 **Figure 2.** Four fluorescence components identified by our PARAFAC model. Components were identified
 288 as (a) shorter-wavelength visible-emitting humic-like (VIS-humic), (b) longer-wavelength VIS-humic,
 289 (c) UV-emitting humic-like (UV-humic), and (d) protein-like.

290 **Table 2. PARAFAC Components Identified in this Study and their Probable Sources.**

Component Number	Component Name	Excitation maximum (nm)	Emission maximum (nm)	Description	OpenFluor References
C1	VIS-humic-like	245 (350) ^a	456	Terrestrial humic-like	45 matches C1 (Osburn, Boyd, et al., 2016)
C2	VIS-humic-like	245 (400)	514	Terrestrial humic-like Soil fulvic-like	35 matches C5 (Yamashita et al., 2010) C1 (Osburn et al., 2012) C4 (Osburn, Hansel, et al., 2016)
C3	UV-humic-like (marine humic-like)	< 240 (310)	392	Microbial humic-like Ubiquitous, but commonly found in wastewater, estuarine, and marine water	41 matches C2 (Osburn, Boyd, et al., 2016) C2 (Murphy et al., 2011)
C4	Protein-like	275	322	Aromatic amino acid-like (Bianchi et al., 2014; Osburn, Boyd, et al., 2016)	4 matches C4 (Osburn, Boyd, et al., 2016) C4 (Bianchi et al., 2014)

291 ^aWavelength in parentheses is a secondary peak in excitation spectrum

292 2.6 Statistical analyses

293 We used one sample student t-tests to evaluate bioavailability and photoreactivity significance. We used
294 two-way ANOVA combined with Tukey's pairwise differences test to evaluate the initial spectroscopic
295 differences and differences in bioavailability and photoreactivity between sites and seasons. For
296 comparison across the Rhode River sites only, we used one-way ANOVA with Tukey's pairwise
297 differences test to evaluate significance. Statements of marginal means are accompanied by the residual
298 standard error (RSE) used in the Tukey test.

299 3 Results

300 3.1 Initial conditions

301 **Table 3.** *Parameters Initially (at Day 0) for each Site and Incubation*

Site	Incubation	DOC (μM) ^a	acDOM300 (m^{-1})	S_R	$S_{275-295}$ (nm^{-1})	$S_{350-400}$ (nm^{-1})	C1 (RU)	C2/C1	C3/C1	C4/C1
Upper MC	16-6/Jun 2016	N/A	20.5	1.03	-0.0186	-0.0179	1.12	0.32	0.72	0.14
Lower MC	16-6/Jun 2016	N/A	11.9	1.09	-0.0190	-0.0175	0.55	0.34	0.85	0.24
SERC Dock	16-7/Jul 2016	312 (4)	7.70	1.27	-0.0212	-0.0167	0.34	0.42	1.0	0.38
RR Mouth	16-6/Jun 2016	N/A	6.23	1.49	-0.0200	-0.0134	0.20	0.38	1.1	0.54
GCReW	16-7/Jul 2016	650 (15)	36.7	0.92	-0.0149	-0.0163	1.56	0.37	0.67	0.13
	16-8/Oct 2016	516 (3)	26.5	0.88	-0.0148	-0.0168	1.17	0.38	0.67	0.11
	17-1/Jan 2017	497 (9)	25.0	0.82	-0.0140	-0.0170	0.94	0.37	0.61	0.13
Jug Bay	16-7/Jul 2016	377 (10)	22.0	0.78	-0.0139	-0.0179	1.12	0.27	0.82	0.20
	16-8/Oct 2016	497 (11)	20.4	0.84	-0.0152	-0.0182	1.20	0.29	0.86	0.22
	17-1/Jan 2017	N/A	9.7	0.85	-0.0160	-0.0188	0.56	0.26	0.95	0.30
Sweet Hall	16-8/Oct 2016	610 (2)	41.6	0.79	-0.0135	-0.0167	1.60	0.33	0.61	0.10
	17-1/Jan 2017	403 (7)	20.3	0.84	-0.0143	-0.0170	0.84	0.32	0.70	0.16
Taskinas	16-7/Jul 2016	570 (2)	30.9	0.89	-0.0150	-0.0169	1.47	0.34	0.63	0.10
	16-8/Oct 2016	497 (5)	22.5	0.91	-0.0160	-0.0176	1.20	0.34	0.65	0.10
	17-1/Jan 2017	N/A	17.4	0.89	-0.0156	-0.0175	0.80	0.34	0.63	0.12

302 *Note.* Measurements performed on GF/F filtrate, equivalent to the 0.7 μm size fraction.303 ^a Standard deviation for DOC measurements listed in parentheses.304 In the Rhode River sub-estuary, DOC concentrations decreased downstream from the marsh, from 650
305 μM at GCReW to 312 μM at the SERC Dock (Table 3). CDOM absorption (acDOM300) decreased down-

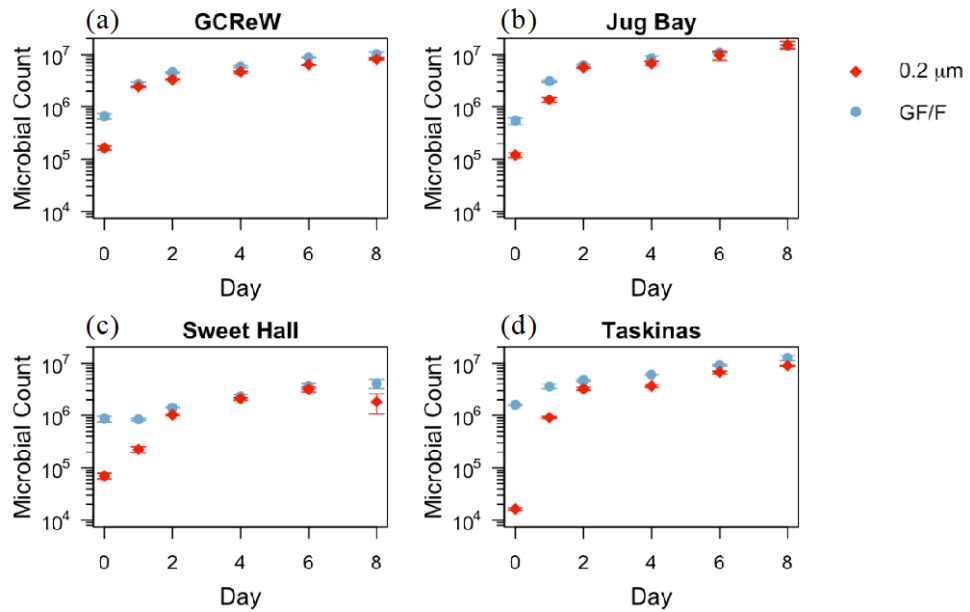
306 estuary by a factor of 6, from 36.7 at GCReW to 6.23 m⁻¹ at the Rhode River Mouth. S_R increased down-
307 estuary, due to both the increase in S₂₇₅₋₂₉₅ and the decrease in S₃₅₀₋₄₀₀ with distance from terrestrial sites.
308 CDOM fluorescence also decreased, particularly the VIS-humic-like components (C1 and C2). Both C1
309 and C2 were highest at GCReW (the marsh end-member) and they both decreased, proportionally, down-
310 estuary with distance from terrestrial DOM sources. As a result, there was no spatial trend in the C2/C1
311 ratio (Table 3). The marine-humic-like (C3) and protein-like (C4) components also decreased down-
312 estuary but to a lesser degree relative to C1 and C2, resulting in an increase in the C3/C1 and C4/C1 ratios
313 down-estuary from 0.72 to 1.1 and from 0.14 to 0.54, respectively (Table 3).

314 Comparing CDOM properties across marshes, the largest CDOM absorption and fluorescence signals
315 were measured at the freshwater Sweet Hall marsh system in October 2016 (aCDOM300 = 41.6 m⁻¹ and C1
316 = 1.60 RU) (Table 3). During the same month, aCDOM300 and C1 varied only slightly across the other three
317 marsh systems (in a narrow range of 20.4-26.5 m⁻¹ and 1.17-1.20 RU, respectively). Dominated by non-
318 persistent emergent marsh vegetation, and with the strongest anthropogenic influence, the Jug Bay system
319 showed some unique marsh CDOM characteristics (Table 3). Lower aCDOM300 and C1 fluorescence were
320 measured in Jug Bay, particularly during the winter (9.7 m⁻¹ and 0.56 RU, respectively), compared to the
321 other marshes (aCDOM300 and C1 in the range of 17.4-25 m⁻¹ and 0.8-0.94 RU, respectively). Jug Bay also
322 had a significantly steeper S₃₅₀₋₄₀₀ compared to GCReW and Sweet Hall ($P < 0.05$), and the highest ratios
323 of the marine:humic (C3/C1) and protein:humic (C4/C1) fluorescence components ($P < 0.05$), particularly
324 during the winter (Table 3).

325 The seasonal variation in CDOM absorption and fluorescence magnitude was pronounced and consistent
326 across systems (Table 3). Both CDOM absorption (aCDOM300) and CDOM fluorescence (particularly C1
327 and C3) decreased considerably from summer to winter for all the marsh sites ($P < 0.05$) and particularly
328 for the freshwater marshes (i.e., Sweet Hall and Jug Bay) where aCDOM300 decreased by more than a factor
329 of two from October to January. Interestingly, compared to CDOM absorption and fluorescence
330 magnitude, the CDOM absorption and fluorescence spectral shape (proxies for CDOM composition)
331 showed considerably less seasonal variability. Specifically, the absorption spectral slopes S_R and S₂₇₅₋₂₉₅
332 and the fluorescence ratios C2/C1, C3/C1, and C4/C1 did not show any statistically significant differences
333 seasonally ($P > 0.1$). Yet, initial values of S₃₅₀₋₄₀₀ for all marsh sites were statistically significantly steeper
334 in the winter than the other months ($P < 0.05$) (see discussion in section §4.5).

335 3.2 Microbial growth

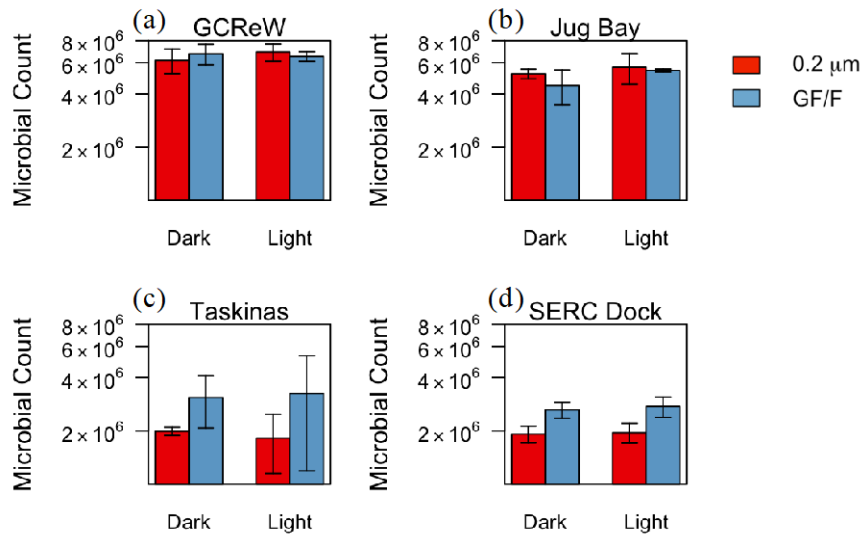
336 Microbial cell count was sampled daily over 8 days for the dark incubations in October 2016, using 0.2
337 μm and GF/F filtrate from all four marsh sites. Although the initial bacterial counts in 0.2 μm filtrate were
338 1-2 orders of magnitude lower than the GF/F filtrate, bacterial growth in the 0.2 μm filtrates was rapid,
339 such that the cell count was close to that in the GF/F filtrate after 1-2 days and remained similar to the
340 GF/F treatments thereafter for all four marsh sites (Figure 3). As a result, for the majority of the parameters
341 analyzed here (e.g., aCDOM300, S_R, S₂₇₅₋₂₉₅, S₃₅₀₋₄₀₀, C3 and C4) the 14-day “control” treatment showed
342 changes that were very similar to and not significantly different than the 14-day microbial-only incubation
343 ($P > 0.05$). The change in DOC was only significantly different ($P < 0.05$) between the two treatments at
344 GCReW and Jug Bay.



345

346 **Figure 3.** Microbial counts per mL for a microbial growth dark incubation test conducted in July 2016 for
 347 the four marsh sites. Error bars represent the standard deviation between three replicate measurements.

348 In July 2016, microbial counts were made for both 0.2 μm and GF/F filtrates after the 7-day light
 349 incubation and 7-day dark incubation. Similar to the dark incubations from October 2016, the final counts
 350 in the 0.2 μm light filtrates were close to those in the GF/F filtrates, varying from 56% to 106% of the
 351 count in the GF/F filtrate (average 84%, standard deviation, SD = 25%) (Figure 4). Moreover, microbial
 352 counts in the 7-day light exposures of GF/F filtrates were the same or greater than the final counts after 7
 353 days in the dark (mean Light/Dark 107%, SD = 10%). This shows that the modest UV irradiance in the
 354 light exposures did not significantly inhibit microbial growth. Similar results were obtained in a second
 355 set of counts made for incubations in January 2017 (data not shown). Given the influence of microbial
 356 activity in the 0.2 μm filtrates, the changes in DOC and optical properties during light exposure of these
 357 samples were not considered measures of photochemical degradation alone. Instead, we only present the
 358 combined PB+MD treatment (GF/F filtrate), and thus have no photobleaching-only treatment. While the
 359 observed microbial growth in the 0.2 μm filtrate did not allow to address the impact of photobleaching
 360 alone, the combined PB+MD treatment is more representative of natural conditions, since photochemical
 361 degradation and microbial degradation co-occur in the natural environment.



362

363 **Figure 4.** Microbial counts per mL for four sites in October 2016 after 7 days with or without light
 364 exposure for either $0.2 \mu\text{m}$ or GF/F filtrate. Error bars show the standard deviation for four replicate bottles
 365 (dark) and three replicate bottles (light).

366

3.3 Microbial degradation

367 DOC decreased for all marsh sites over the 14-day dark incubation by, on average, 5.5% ($SD = 5.4\%$).
 368 Jug Bay had a significantly greater relative loss compared to the other three marsh sites (marginal means
 369 11.7% vs. 2.7-4.2% over 14 days, on average, $RSE = 3.0\%$) ($P < 0.01$) (Figure 5a). The DOC loss was
 370 also significantly lower for samples collected in July 2016 than October 2016 and January 2017 ($P <$
 371 0.01).

372 **Table 4.** Average Percent Change for All Incubations and Sites (Marsh and Rhode River), for each
 373 Measured Parameter

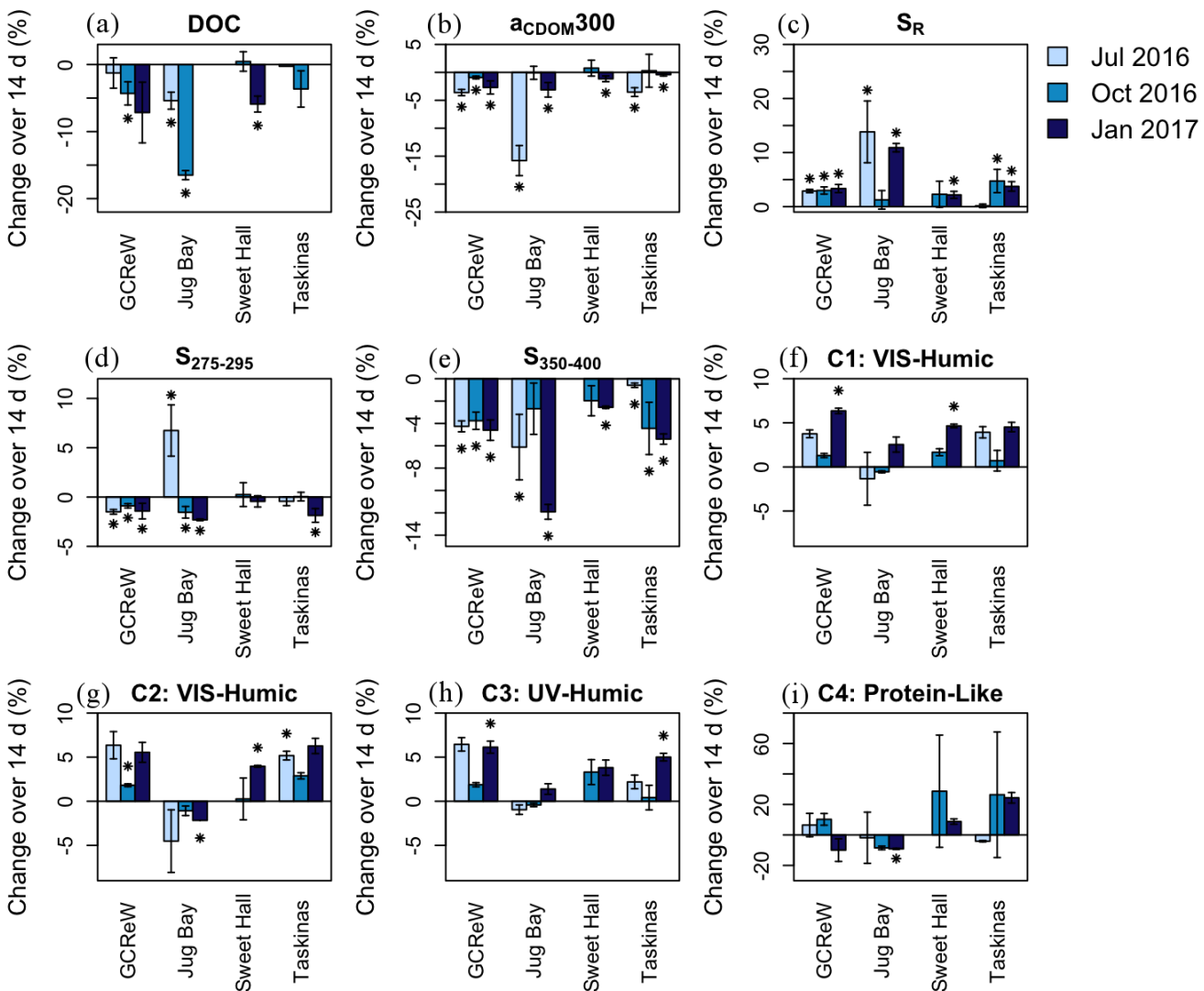
Treatment	Site n ^a	a _{CDOM300}	S _R	S ₂₇₅₋₂₉₅	S ₃₅₀₋₄₀₀	C1	C2	C3	C4
MD (14 d)	Marsh	-2.8% (4.6%)	4.4% (4.5%)	-0.3% (2.6%)	-4.4% (3.1%)	2.5% (2.4%)	2.2% (3.8%)	2.7% (2.5%)	6.5% (19.2%)
	RR	-0.5% (7.7%)	2.1% (5.4%)	-1.1% (5.4%)	-2.8% (9.4%)	4.9% (1.1%)	5.2% (2.9%)	7.2% (3.2%)	39.8% (47.1%)
	20, 10								
PB+MD (7 d)	Marsh	-57.0% (4.1%)	105.1% (23.4%)	63.3% (8.7%)	-19.6% (7.6%)	-79.1% (4.3%)	-51.2% (6.0%)	-78.6% (5.4%)	-8.3% (23.0%)
	RR	-53.4% (3.3%)	66.7% (15.8%)	48.6% (5.2%)	-10.0% (10.5%)	-70.5% (5.8%)	-36.4% (8.8%)	-77.5% (5.1%)	-19.4% (15.0%)
	15, 10								
MD after PB (7 d)	Marsh	-6.0% (6.3%)	-3.7% (5.0%)	-0.4% (4.0%)	3.7% (5.0%)	17.9% (8.5%)	-1.8% (6.6%)	18.8% (11.8%)	3.6% (12.6%)
	33, 21								

RR	-0.6%	-4.2%	-3.4%	0.9%	16.5%	2.7%	28.5%	0.8%
15, 10	(5.9%)	(3.1%)	(2.4%)	(3.7%)	(2.7%)	(4.2%)	(10.3%)	(6.4%)

374
375 Note. The four marsh sites in Figure 2a averaged across all three seasons for “Marsh,” with the exception
376 of Sweet Hall in the Summer 2016, which was not sampled. The five Rhode River sites in Figure 2b,
377 including GCReW, averaged during the Summer 2016 for “RR”. Negative values indicate a net loss and
378 positive values a net gain. Standard deviations are listed below the mean in parentheses.

379 ^a The total number of samples, including incubation replicates, averaged for the absorption indices and
380 fluorescence indices, respectively

380
381



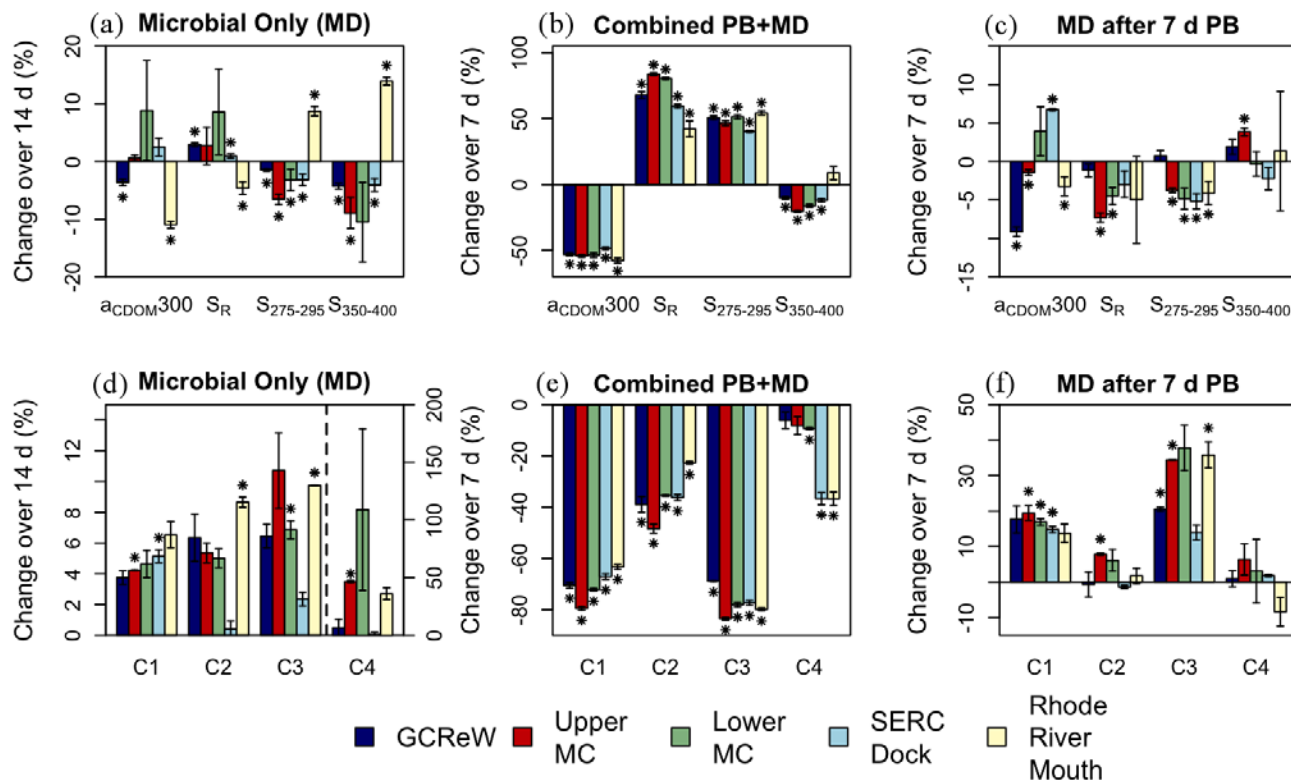
382

383 **Figure 5.** Change in optical properties and dissolved organic carbon (DOC) after 14 d of dark incubations
384 performed on GF/F filtrate during July 2016, October 2016, and January 2017. Error bars represent the

385 standard deviation between replicate bottles. Asterisks represent a significant difference between the
 386 percent change and zero (t.test, $P < 0.05$).

387 The absorption (acdOM300) of marsh exported CDOM consistently decreased over the 14-day incubation
 388 (Figure 5b), with Jug Bay showing significantly ($P < 0.05$) greater loss of acdOM300 compared to the other
 389 three marsh sites (marginal means 6.3% vs. 0.3-2.4% over 14 days, RSE 2.9%) (Figure 5b). Overall, S_R
 390 increased during microbial degradation, with Jug Bay, again, showing a significantly higher increase in
 391 S_R compared to the other marshes (marginal means 8.7% vs. 2.2-3.1% over 14 days, on average, RSE =
 392 3.6%) ($P < 0.01$). In all cases, the increase in S_R was the result of a decrease in both $S_{275-295}$ and $S_{350-400}$,
 393 with a larger decrease in $S_{350-400}$ (Figures 5c-e and 6a). Jug Bay also had a significantly higher loss in $S_{350-400}$
 394 than the other marsh sites (marginal means 6.9% vs. 2.3-4.2% over 14 days, on average, RSE = 2.3%)
 395 ($P < 0.05$). Microbial degradation had, overall, a smaller impact on the absorption of estuarine CDOM
 396 collected from the Rhode River, resulting in both an increase and a decrease in acdOM300 across the
 397 salinity gradient (Figure 6a).

398 For all sub-estuary and marsh sites, the humic-like fluorescence components (C1, C2, and C3) increased
 399 over the 14-day microbial incubation (with the exception of Jug Bay) (Figure 5f-i and Figure 6d). The
 400 average increase in C1 for all marsh sites was 2.5% after 14 days ($SD = 2.4\%$) (Table 4), with the greatest
 401 increase occurring in January 2017. Across the Rhode River, C1 showed a larger increase at the mouth of
 402 the estuary compared to the GCReW marsh end-member ($P < 0.05$). Similar trends were observed for C2
 403 and C3. Jug Bay was the only marsh system where the humic-like components decreased during the July
 404 and October 2016 incubations. Similarly, while the protein-like component (C4) showed a substantial
 405 increase for all the Rhode River sites (by 39.8% on average, $SD = 47.1\%$) and most of the marsh sites, it
 406 consistently decreased at Jug Bay (Figure 6d, Figure 5i).

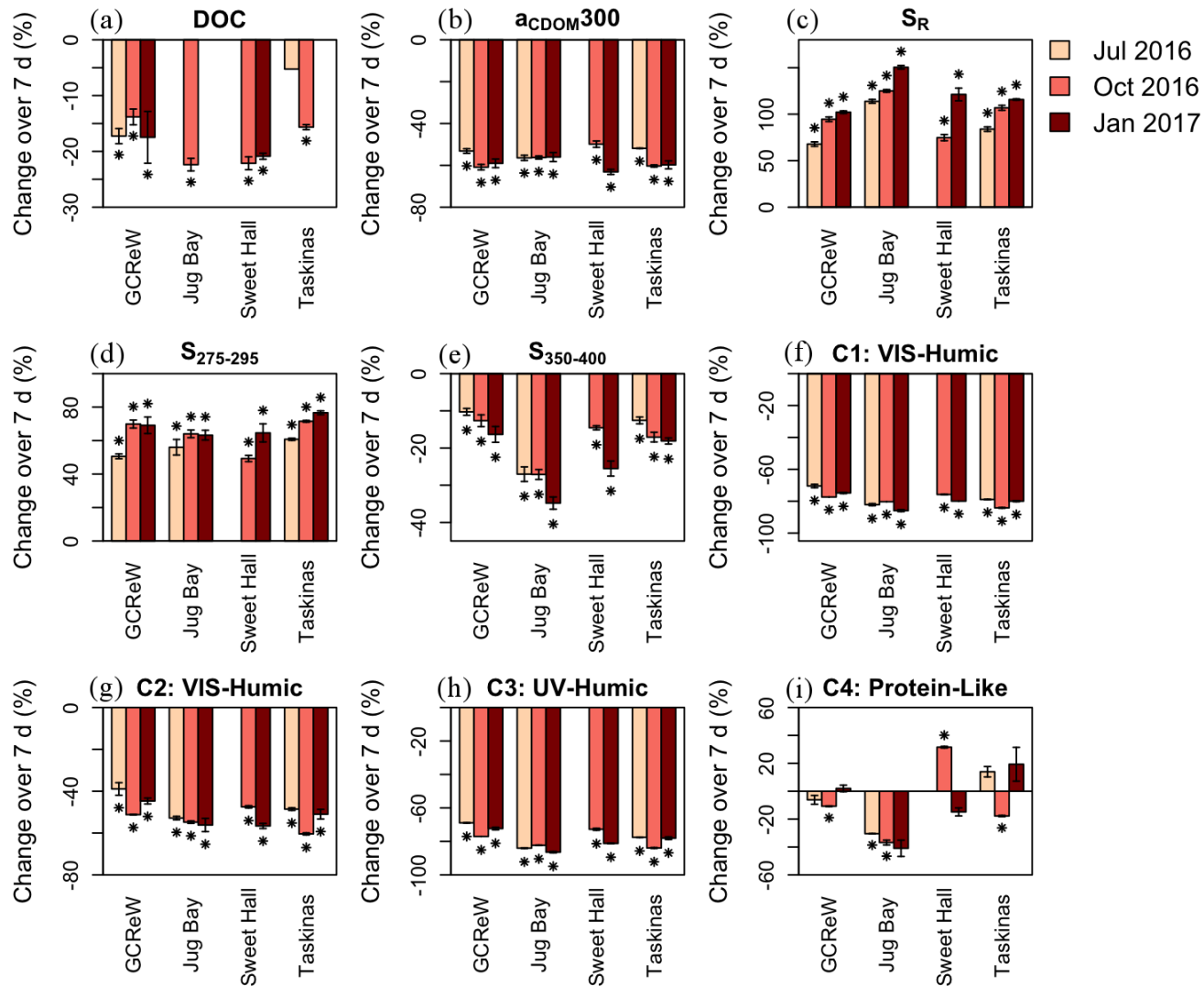


407
 408 **Figure 6.** Changes to CDOM absorption properties (a, b, and c) and CDOM fluorescence properties (d, e,

409 and f) for the microbial-only treatment (a and d), the combined photobleaching and microbial treatment
 410 (b and e), and the microbial treatment after 7 d of photobleaching (c and f) for the Rhode River sub-estuary
 411 sites. Sites are ordered along the salinity gradient, starting with the marsh end-member (GCReW) and
 412 ending with the estuarine end-member (Rhode River Mouth). The C4 component in the microbial-only
 413 treatment (d) is plotted on a different scale than the other 3 components. Error bars represent the standard
 414 deviation between replicate bottles. Asterisks represent a significant difference between the percent
 415 change and zero (t.test, $P < 0.05$).

416 3.4 Combined photobleaching and microbial degradation

417 Microbial degradation coupled with photobleaching resulted in a decrease in DOC concentrations for all
 418 marsh sites by 17.8% on average ($SD = 4.6\%$) over the 7-day light incubation (Table 4 and Figure 7a).
 419 Taskinas had a significantly lower overall DOC loss compared to Jug Bay and Sweet Hall ($P < 0.01$),
 420 though there were no significant differences seasonally.



421
 422 **Figure 7.** Change in optical properties and dissolved organic carbon (DOC) after 7 d of light incubations
 423 performed on GF/F filtrate (combined photobleaching and microbial, “PB+MD”) during July 2016,

424 October 2016, and January 2017. Error bars represent the standard deviation between replicate bottles.
425 Asterisks represent a significant difference between the percent change and zero (t.test, $P < 0.05$).

426 Similar to microbial degradation alone, CDOM absorption (acDOM300) decreased for all sites during the
427 combined photobleaching and microbial degradation treatment, but to a much greater extent (by 56.0%
428 over 7 days on average, $SD = 4.3\%$), ranging from a loss of 48.4% at the SERC Dock in July 2018 to
429 63.1% at Sweet Hall in January 2017 (Figure 6b and Figure 7b). There was little variation in the change
430 in acDOM300 across the estuarine gradient or between marshes ($P > 0.05$). There was, however, a seasonal
431 dependence, with a significantly higher relative loss in acDOM300 in January (59.5% over 7 days, on
432 average, $SD = 3.1\%$) compared to July (52.5% over 7 days, on average, $SD = 3.1\%$) ($P < 0.01$). S_R showed
433 a consistent and significant increase (by 94.8% over 7 days for all sites on average, $SD = 27.9\%$, $P <$
434 0.01), as a result of an increase in $S_{275-295}$ and a decrease, or no change, in $S_{350-400}$ (Figure 6b and Figure
435 7e). Across the Rhode River estuarine gradient, the greatest percent increase in S_R occurred at Upper
436 Muddy Creek (83.7% over 7 days), with a monotonic decrease in S_R change downstream towards the
437 mouth (Figure 6b). The percent increase in S_R was also significantly higher in the winter compared to the
438 fall and summer and in the fall compared to the summer ($P < 0.01$) (Figure 7c). Jug Bay had a greater
439 increase in S_R (129.8% over 7 days, on average, $SD = 16.3\%$, $P < 0.01$) and GCReW an overall smaller
440 increase in S_R (88.2% over 7 days, on average, $SD = 15.7\%$ $P < 0.01$). The increase in $S_{275-295}$ was
441 significantly greater at Taskinas than both Jug Bay and Sweet Hall ($P < 0.01$). Furthermore, there was a
442 significantly lower percent increase in $S_{275-295}$ in the summer compared to the fall and winter ($P < 0.01$)
443 (Figure 7d). Jug Bay and GCReW also had a significantly greater (29.6% over 7 days, on average, $SD =$
444 4.1%) and lower (13.1% over 7 days, on average, $SD = 3.0\%$) percent loss in $S_{350-400}$, respectively, than
445 the other sites ($P < 0.01$), except for Taskinas which showed no significant difference compared to
446 GCReW ($P > 0.05$).

447 Combined photobleaching and microbial degradation resulted in a significant decrease in all the humic-
448 like fluorescence components ($P < 0.01$), with the greatest losses occurring in the shorter-wavelength VIS-
449 humic-like component (C1) and the marine-humic-like component (C3) (Figure 6e and Figure 7f and h).
450 For the Rhode River sites, the percent loss of C1 was greatest in terrestrially-sourced sites such as Upper
451 Muddy Creek (loss of 79.5% over 7 days). This loss decreased down-estuary, with the lowest percent loss
452 occurring at the Rhode River Mouth (loss of 63.2% over 7 days). The decrease in C1 and C3 was
453 significantly lower at the GCReW marsh compared to Upper Muddy Creek, the “non-marsh terrestrial”
454 site ($P < 0.01$). Furthermore, Upper Muddy Creek had a significantly greater percent loss in all humic-
455 like components (C1, C2, and C3) compared to the other sites ($P < 0.01$). GCReW also had a significantly
456 lower percent loss of the three humic-like components compared to Jug Bay and Taskinas ($P < 0.05$). In
457 general, the protein-like component (C4) varied more than the humic-like components. There was a
458 consistent decrease in C4 with combined photobleaching and microbial degradation at Jug Bay, in all
459 seasons (Figure 7i) ($P < 0.1$).

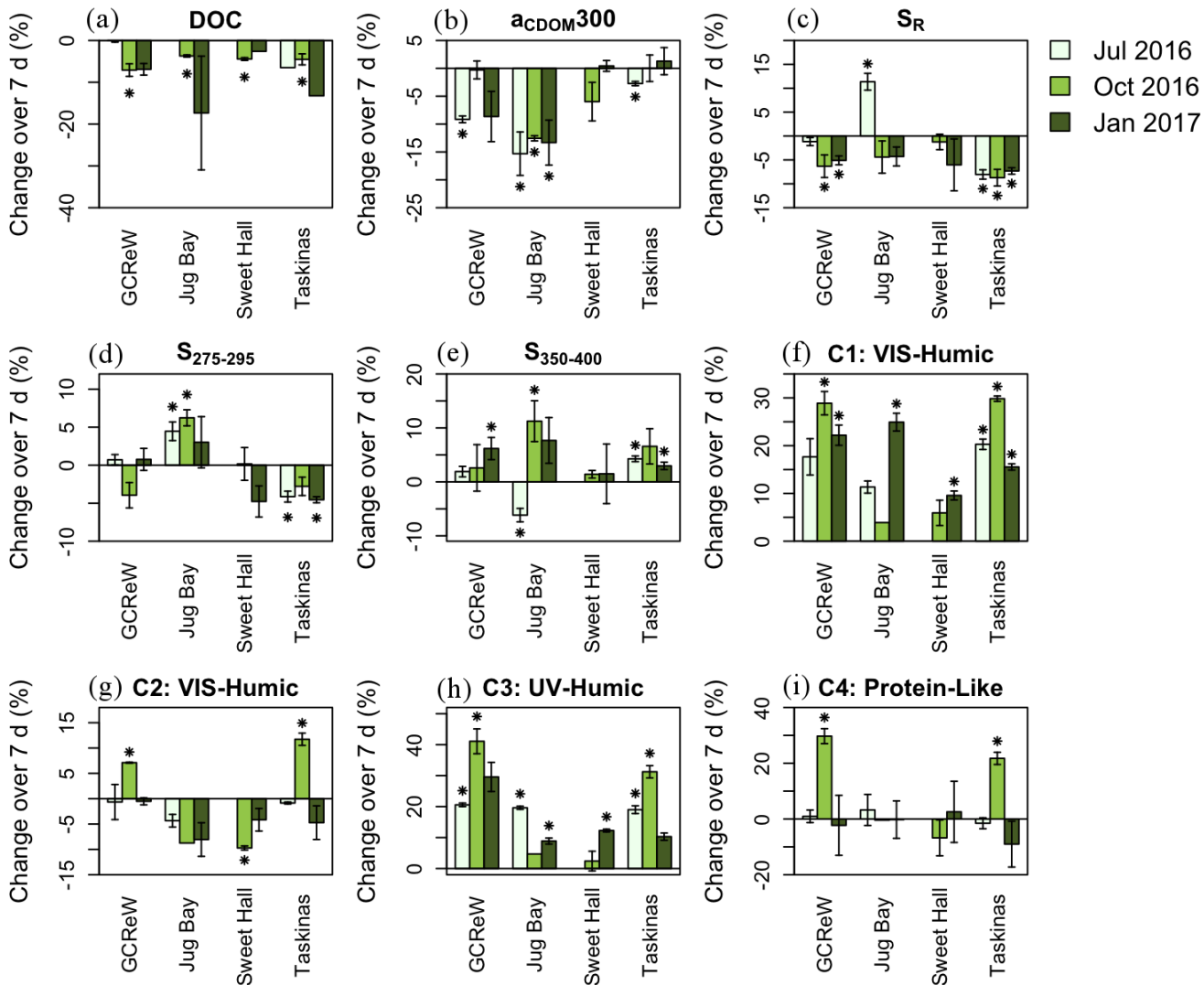
460 3.5 Effects of photobleaching on microbial degradation

461 DOC decreased for all marsh sites by, on average, 5.9% ($SD = 5.6\%$) over the 7-day dark incubation after
462 light exposure (Table 4 and Figure 8a); this was greater than the loss of DOC from microbial degradation
463 alone, which was 5.5% ($SD = 5.4\%$) over the twice as long period of 14 days. There were no significant
464 differences in DOC loss between sites or seasons ($P > 0.05$).

465 The average decrease in acDOM300 for the marsh sites was 6.0% ($SD = 6.3\%$) over the 7-day dark
466 incubation after photobleaching, which is considerably larger than the average decrease of 2.8% ($SD =$

467 4.6%) over the longer 14-day microbial-only incubations (Table 4). Jug Bay had a significantly greater
468 loss in aCDOM300 compared to the other marsh sites (marginal means 13.7% vs. 0.5-6.0% over 7 days,
469 RSE = 3.5%, $P < 0.01$) (Figure 8b). Contrary to the microbial-only and combined photochemical and
470 microbial incubations where S_R increased, in the microbial degradation incubations after photobleaching
471 S_R consistently decreased by, on average, 4.2% (SD = 3.1%) for the Rhode River sites and 5.8% (SD =
472 2.9%) for the marsh sites (Table 4). This decrease in S_R was mostly the result of a decrease in $S_{275-295}$ and
473 an increase in $S_{350-400}$. CDOM from the Jug Bay marsh, however, showed different results, with both $S_{275-295}$
474 and $S_{350-400}$ increasing during the microbial incubation after photobleaching, except in July 2016 when
475 $S_{350-400}$ decreased, resulting in an increase in S_R (Figure 8c,e).

476 Overall, exposure to light increased the subsequent microbial production of CDOM fluorescence (Figure
477 8f-i), especially for the humic-like peaks C1 and C3 that both consistently increased with microbial
478 degradation after photobleaching to a greater extent than by microbial degradation alone. Specifically, 7
479 days of microbial degradation following 7 days of photobleaching resulted in an increase in C1 by 16.5%
480 (SD = 2.7%), on average, in the Rhode River sites and by 17.9% (SD = 8.5%) in the marsh sites (Table
481 4). This is considerably higher than the 4.9% (SD = 1.1%) and 2.5% (SD = 2.4%) increase for estuarine
482 and marsh sites, respectively, in the 14-day microbial-only incubations. Similarly, component C3
483 increased by 28.5% (SD = 10.3%) for the Rhode River sites and by 18.8% (SD = 11.8%) for the marsh
484 sites, compared to just 7.2% (SD = 3.2%) and 2.7% (SD = 2.5%) increase, respectively, in the 14-day
485 microbial-only incubations. C4 was much more variable, with most incubations showing no significant
486 changes ($P > 0.1$).



487

488

489

490

491

492

493

494

495

496

Figure 8. Change in optical properties and dissolved organic carbon (DOC) over 7 d of dark incubations after 7 d of light incubations performed on GF/F filtrate during July 2016, October 2016, and January 2017. Error bars represent the standard deviation between replicate bottles. Asterisks represent a significant difference between the percent change and zero (t.test, $P < 0.05$).

Along the estuarine gradient, the UV-humic-like peak C3 showed overall the largest increase with microbial degradation after photobleaching, both for the terrestrial (Upper and Lower Muddy Creek) and the estuarine (Rhode River Mouth) end-members (Figure 6f). The VIS-humic-like peak, C1, also showed a consistent increase with microbial degradation after photobleaching that monotonically decreased, however, with increasing salinity along the estuary.

497

4 Discussion

498

4.1 CDOM properties at the wetland-estuary interface

499

500

Our measurements in the Rhode River system showed a decreasing gradient in highly absorbing CDOM and humic-like fluorescence with increasing distance from the marsh and watershed. These gradients are

501 driven by dilution of terrestrial (including marsh) CDOM sources, as well as removal, production and
 502 transformation of CDOM within the estuary. The steeper gradient of the two visible humic-like
 503 fluorescence components (C1 and C2) compared to the UV-humic-like (C3) and protein-like (C4)
 504 components from the GCReW marsh to the Rhode River mouth initially (Table 3) indicate either the
 505 preferential loss of the longer wavelength, higher molecular weight humic-like components relative to C3
 506 and C4 down-estuary, or additional sources of C3 and C4 down-estuary. Since C3 and C4 are both
 507 associated mostly with microbially-processed material (Coble, 1996; Fellman et al., 2010) and C1 and C2
 508 are associated mostly with terrestrial sources (Coble, 1996; Fellman et al., 2010; Wagner et al., 2015;
 509 Yamashita et al., 2010), it is likely that C3 and C4 fluorescence down-estuary is supplemented by
 510 relatively stronger autochthonous production. This is consistent with the results from our microbial
 511 incubation experiments showing a larger increase in C3 and C4 fluorescence relative to C1 and C2 for
 512 both estuarine and marsh-exported CDOM (MD treatment, Table 4). Moreover, C3 fluorescence showed
 513 the largest increase in our microbial incubations after photobleaching (MD after PB treatment, Table 4).

514 The decrease in $a_{CDOM300}$ (by more than a factor of 3) and increase in S_R (from 1.03 to 1.49) with distance
 515 from the marsh endmember suggests a decrease in the molecular weight and aromaticity of CDOM across
 516 this marsh-estuarine gradient (Table 3), in agreement with other studies (Hernes, 2003; Helms et al.,
 517 2008a; Tzortziou et al., 2008; 2011; Yamashita et al., 2008; Dalzell et al., 2009; Fellman et al., 2011). For
 518 samples collected along a transect in the Delaware Estuary, Helms et al. (2008) proposed that the optics
 519 down-estuary were the result of: the mixing of low S_R (terrestrial) CDOM with high S_R (autochthonous
 520 or photobleached terrestrial) CDOM, increasing $S_{275-295}$ down-estuary (photobleaching impacts), and
 521 decreasing $S_{350-400}$ down-estuary (microbial impacts). While the salinity gradient in Helms et al. (2008)
 522 had a much larger range than the Rhode River (i.e., 0 to 40 versus 6 to 9 salinity), nonconservative mixing
 523 in CDOM optical properties such as $a_{CDOM440}$ and $S_{290-750}$ was previously reported for the Rhode River
 524 along transects from the marsh endmember to the mouth of the estuary (Tzortziou et al., 2011), suggesting
 525 a sink for highly-absorbing CDOM. J. B. Clark et al., (2020) showed this sink to be phototransformation;
 526 they estimated that about half of the total DOC input from the marsh and watershed to the Rhode River is
 527 photochemically transformed to a more biologically labile (and less absorbing) DOC pool. Therefore, in
 528 the summer, the GCReW marsh exports high molecular weight (low S_R) and strongly-absorbing (high
 529 $a_{CDOM300}$) CDOM to the surrounding estuary (Tzortziou et al., 2008, 2011). The marsh-exported CDOM
 530 is then photobleached and microbially degraded (J. B. Clark et al., 2020), mixed with terrigenous CDOM
 531 from Muddy Creek, and diluted with down-estuary water characterized by lower $a_{CDOM300}$ and higher S_R
 532 (Tzortziou et al., 2011).

533 Consistent CDOM quality in the Rhode River estuary inter-annually suggests consistent CDOM sources
 534 and transformation pathways. Our measured S_R of 0.92 at GCReW and 1.27 at the SERC Dock in July
 535 2016 were remarkably consistent with the S_R values of 0.9 at GCReW and 1.29 at the SERC Dock reported
 536 for July 2008 measurements in Tzortziou et al. (2011). These observations, conducted in same season and
 537 tidal stage but different years, suggest consistency in the relative contribution of different CDOM sources
 538 and transformation pathways across this marsh-estuarine gradient. Tzortziou et al. (2008), measured
 539 $a_{CDOM300}$ of 35.7 m^{-1} and 54.2 m^{-1} (both having absorption spectral slopes $S_{290-750}$ of 0.0143 nm^{-1}) for
 540 two asymmetrical low-tides (i.e., GCReW-exported CDOM) on July 2004. While one of these values is
 541 similar to our measurement of 36.7 m^{-1} for $a_{CDOM300}$ at GCReW in July 2016, the other is not. Ultimately,
 542 this demonstrates that while down-estuary gradients of optical parameters that are proxies for CDOM
 543 composition (i.e., S_R , $S_{290-750}$) remain overall consistent, the magnitude of proxies that are driven by both
 544 CDOM amount and composition (i.e., $a_{CDOM300}$) vary on interannual, seasonal, and even daily timescales,
 545 especially during asymmetrical tidal cycles (Tzortziou et al., 2008).

546

4.2 CDOM as a function of source and season

547

Across the marsh sites, DOC concentrations, $a_{CDOM300}$, and contributions of the four PARAFAC fluorescence components decreased from July to January, in some cases by a factor of two or more, thus indicating greater marsh export of carbon-rich, more absorbing and strongly fluorescent CDOM in the summer compared to the winter (Table 3). Similar seasonal changes have been reported in previous studies (Fellman et al., 2008; Osburn et al., 2015; Shultz et al., 2018; Stedmon & Markager, 2005; Tzortziou et al., 2008). Seasonally, the contributions of various CDOM sources at the marsh-estuary interface may vary; for example, in the winter compared to the summer, there is likely a lesser contribution of CDOM from marsh plant leachates; however, DOM contributions of from fresh plant materials in other marsh systems have been shown to be minor relative to soil (C. D. Clark et al., 2008). Moreover, due to the temperature-dependence of soil CDOM export in similar systems such as rivers (Shultz et al., 2018), the contribution of wetland-soil CDOM is also likely lower in the winter. Since CDOM absorption and fluorescence quality indices (ratios of fluorescence components, S_R , and $S_{275-295}$), showed considerably smaller changes seasonally and inter-annually relative to the quantity of marsh DOM export, it is likely that marsh-exported CDOM mostly originates from marsh soil porewater rather than plant leachates, as suggested in C. D. Clark et al. (2008). The gradual release of DOM stored in tidal marsh soils reduces much of the seasonal and inter-annual variability in the quality of DOM exported from temperate marshes relative to the strong seasonal and inter-annual variability in the ultimate source of these compounds (i.e., plant biomass), thus buffering marsh DOM export.

565

Dominated primarily by non-persistent emergent vegetation and downstream of a major WWTP, Jug Bay differed from the other marsh systems in both CDOM quantity and composition. In the winter, Jug Bay had much lower CDOM absorption and fluorescence (expressed by $a_{CDOM300}$ and C1) compared to the other marshes. This is likely the result of the lack of emergent vegetation at Jug Bay during the winter and a smaller peat reserve and greater mineral content compared to the other marshes (Pinsonneault et al., in review; Swarth et al., 2013). In addition, the observed high contributions of marine-humic-like and protein-like CDOM fluorescence components at Jug Bay compared to the other marshes indicates a greater contribution of microbial CDOM and could be representative of the influence of wastewater treatment effluent at this site, given that the marine humic-like component has been shown to be higher in sewage and wastewater (Guo et al., 2010). Thus, Jug Bay exemplifies the role of both source material (e.g., vegetation type and soil characteristics) as well as environmental characteristics, such as water quality, on CDOM quantity and composition.

577

4.3 Microbial impacts in the 0.2 μ m fraction

578

Many incubation studies assume little to no microbial activity in 0.2 μ m filtrate, despite studies demonstrating the 0.2 μ m filterability and growth of certain microbial communities in experiments even though sterilization of equipment was performed (Liu et al., 2019; Wang et al., 2008). In fact, significant microbial presence in 0.2 μ m filtrate has been observed in inland surface waters (Brailsford et al., 2017; Elhadidy et al., 2016; Wang et al., 2007), coastal water (MacDonell & Hood, 1982; Obayashi & Suzuki, 2019), and groundwater (Luef et al., 2015). Our results showed that while microbial counts in the 0.2 μ m filtrate were about an order of magnitude lower than the GF/F filtrate before the incubation, they approached those in the GF/F filtrate after only 2 days (Figure 3), suggesting the potential for microbial interference in a filtrate that is often assumed to be “sterile.” Microbial counts reported here for 0.2 μ m filtrate are similar to those reported for other aquatic systems such as freshwater lakes and rivers (Liu et al., 2019; Wang et al., 2007). The interference of microbes was further supported by the observed similar trends between the “control” 0.2 μ m 14-day dark incubation and the MD-only 14-day incubation.

590 While UV exposure has also been assumed to inhibit microbial growth, in our incubations low-level UV
 591 light exposure that was mainly composed of long-wavelength UV-A did not inhibit microbial growth as
 592 evidenced by the small difference between the dark and light microbial counts at the end of the 7-day
 593 incubation ($P > 0.1$) (Figure 4). Therefore, the potential for microbial interference in treatments that are
 594 assumed to isolate the impacts of other degradation processes, such as photobleaching, must be
 595 acknowledged. Work addressing potential solutions to bacterial contributions in commonly used “sterile”
 596 fraction sizes (i.e., $0.2 \mu\text{m}$) should be conducted, and microbial counts should be measured for incubations
 597 when possible. Common treatment methods to inhibit microbial growth, for example sodium azide, can
 598 interfere with CDOM optical measurements (Retelletti Brogi et al., 2019) and thus can’t be used for
 599 photobleaching-only experiments that are assessing changes to CDOM optics. Incubations that assume
 600 $0.2 \mu\text{m}$ fractions as “sterile” without the presentation of microbial cell counts or similar evidence of
 601 sterility should be interpreted with caution, as there exists the potential for under- or over-estimation of
 602 degradation processes such as photobleaching, due to the coupled effects of microbial activity.
 603 Photodegradation experiments conducted on very short-time scales may reduce the confounding effects
 604 of microbial growth, and thus should be considered, when possible.

605 4.4 Photobleaching increases CDOM bioavailability

606 Microbial degradation of DOM is affected by numerous factors, such as nutrient availability, microbial
 607 community composition, source material, previous light exposure, and temperature (which was constant
 608 in our experiments); thus, the effects of microbial degradation on marsh-exported CDOM were highly
 609 variable. This variability is particularly apparent when comparing across marshes and seasons. In general,
 610 microbial degradation resulted in increases to CDOM humic-like and protein-like (C4) fluorescence
 611 (Figure 5f-i, Figure 6d and f, and Figure 8f-i), but decreases to CDOM absorption (Figure 5b, Figure 6a
 612 and c, Figure 8b). Similar to other studies, we observed a small (within 10%, Table 4, Figure 5f,h, Figure
 613 6d) increase in the shorter-wavelength VIS- and marine-humic-like fluorescence components (C1 and C3)
 614 of marsh and estuarine CDOM with microbial degradation alone (Cory et al., 2015; Lu et al., 2013; Moran
 615 et al., 2000; Rochelle-Newall & Fisher, 2002), particularly for C3, which is associated with biological
 616 processing. This increase could be the biological transformation of non-colored DOM to colored DOM,
 617 as hypothesized by Rochelle-Newall and Fisher (2002). The observed down-estuary increase in C1
 618 microbial production could be due to the increasing presence of algal-derived DOM down-estuary, which
 619 has been proposed as the non-colored DOM substrate converted into the colored, humic-like CDOM
 620 fluorescence fraction (Rochelle-Newall & Fisher, 2002). The greater increase in C1 microbial production
 621 down-estuary could also be due to greater prior light exposure during transport down-estuary, and
 622 therefore, a greater CDOM bioavailability.

623 Previous exposure to light increased the bioavailability of CDOM at all sites, resulting in a greater loss of
 624 both DOC and acDOM₃₀₀ and a greater production of humic-like CDOM over a shorter incubation time (7
 625 days versus 14 days for the microbial-only incubation). Similar results have been reported for the Ria de
 626 Aveiro estuary (Santos et al., 2014), the Satilla estuary dominated by vascular plant CDOM inputs (Moran
 627 et al., 2000), and an arctic headwater stream (Cory et al., 2015). The bioavailability increase was
 628 particularly prominent in sites where the contributions of terrestrial, humic-like, and aromatic CDOM
 629 were higher, and with less previous exposure to UV-radiation; for example, the bioavailability increase in
 630 C1 was greater in the marsh and watershed sites (GCReW and the Upper Muddy Creek) compared to the
 631 down-estuary sites, since estuarine CDOM has likely undergone substantially more photobleaching
 632 (Tzortziou et al., 2007). Microbial production of C3 increased the most after photobleaching, particularly
 633 in the Rhode River sites. Without previous exposure, microbial production of C3 was only slightly higher

634 than that of C1 (7.2% compared to 4.9% over 14 days for the Rhode River sites); after photobleaching,
 635 however, the increase in C3 during microbial degradation was, on average, almost double that of C1
 636 (28.5% compared to 16.5% over 7 days for the Rhode River sites). Therefore, while photobleaching
 637 stimulates the microbial production of both C1 and C3, the relative increase in C3 is greater. For the marsh
 638 sites, the loss of C2 during microbial degradation after photobleaching was significant, even in sites that
 639 showed no loss with microbial degradation alone; this indicates that photobleaching is allowing for the
 640 microbially-mediated decrease of C2 fluorescence. While fluorescence components C1, C2, and C3
 641 (humic-like) are often described as terrestrially-sourced and associated with wetlands (which they often
 642 are, including in the marshes studied here), our results, consistent with other studies (Medeiros et al., 2017;
 643 Tanaka et al., 2014), demonstrate another source in estuarine systems: microbial production within the
 644 estuary.

645 In general, CDOM absorption ($a_{CDOM300}$) decreased with microbial degradation. This is consistent with
 646 other incubations of terrestrial CDOM (Cory et al., 2015; Moran et al., 2000; Santos et al., 2014), though
 647 increases in CDOM absorption for estuarine and marine CDOM have also been reported (Miller & Moran,
 648 1997; Nelson et al., 2004; Rochelle-Newall & Fisher, 2002; Santos et al., 2014). The observed loss in
 649 $a_{CDOM300}$ during microbial processing was enhanced by previous exposure to light, with a loss of 2.8%
 650 over 14 days in the microbial-only treatment, and 6.0% over half the time (7 days) during the microbial
 651 incubation with prior photobleaching. This is consistent with Miller and Moran (1997), where CDOM
 652 from a coastal salt marsh dominated by *Sporobolus alterniflora* showed no change in $a_{CDOM350}$ by
 653 microbial degradation alone but a 4% decrease by microbial degradation after photobleaching. On the
 654 other hand, in an arctic headwater stream dominated by terrestrial soil CDOM sources, CDOM absorption
 655 and fluorescence increased during microbial incubations after photobleaching (Cory et al., 2015). These
 656 differences indicate the importance of CDOM source when evaluating the impacts of photobleaching on
 657 microbial degradation.

658 4.5 Factors influencing CDOM photoreactivity

659 Our combined photobleaching and microbial incubations highlighted the dominant role of photobleaching,
 660 but also the importance of simultaneous microbial processing, in shaping certain CDOM optical properties
 661 in estuarine waters. The substantial loss of all three humic-like fluorescence components and $a_{CDOM300}$
 662 (by > 50%, Table 4) in the PB+MD treatment is consistent with previous studies on the impacts of
 663 photobleaching alone (Aulló-Maestro et al., 2016; Cory et al., 2015; Helms et al., 2008; Tzortziou et al.,
 664 2007), indicating the dominant role of photobleaching as the main CDOM quality transformation
 665 mechanism for the specific samples. This is further supported by the much larger change in all CDOM
 666 optical properties over the 7-day combined incubation compared to the microbial treatments with and
 667 without previous light exposure. Yet, the influence of microbial degradation in the combined treatments
 668 may still be important, especially for some parameters. Although both microbial and photochemical
 669 degradation decreased marsh and estuarine CDOM absorption, photobleaching resulted in opposite shifts
 670 in CDOM fluorescence, with humic-like components decreasing during photochemical degradation and
 671 increasing during microbial processing. The increase in humic-like CDOM fluorescence (i.e., C1 and C3)
 672 during microbial degradation after prior photobleaching was substantial compared to the fluorescence loss
 673 during the combined photobleaching and microbial treatment (Table 4), especially compared to the
 674 differences between sites and seasons (Figure 6e compared to Figure 6f and Figure 7f-h compared to
 675 Figure 8f-h). Therefore, the loss of the humic-like fluorescence in the combined photobleaching and
 676 microbial treatment is likely much lower than it would be for photobleaching alone, given the offset in
 677 loss due to the simultaneous microbial production; furthermore, trends in the humic-like fluorescence

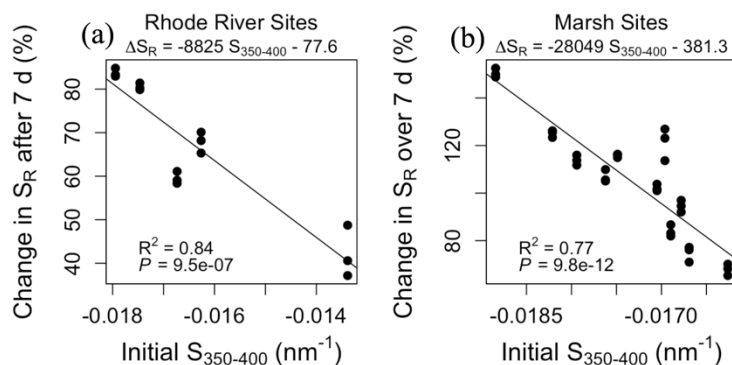
678 components during the combined photochemical and microbial treatment cannot be confidently attributed
 679 to photobleaching alone, and thus the change in humic-like fluorescence in this study may not be a good
 680 proxy for the amount of photobleaching. S_R , on the other hand, was both the parameter that changed the
 681 most during photobleaching and was also not as highly impacted by microbial degradation (Table 4). In
 682 fact, the amount of change in S_R during microbial degradation after previous light exposure was in many
 683 cases less than the difference between sites or seasons in the combined photochemical and microbial
 684 treatment (Figure 6b compared to Figure 6c and Figure 7c compared to Figure 8c). Thus, the change in S_R
 685 may be a good proxy to gauge the amount of photobleaching, despite the simultaneous influence of
 686 microbial processing.

687 CDOM photoreactivity is driven by both CDOM source and prior light exposure. For the Rhode River,
 688 the greatest increase in S_R occurred in the terrestrial sites, where the contributions of CDOM with
 689 presumed higher aromaticity (GCReW, Upper and Lower Muddy Creek) were greatest; the lowest
 690 increase occurred in the estuarine end-member (Rhode River Mouth) (Figure 6b and e), which had the
 691 lowest contribution of terrestrial CDOM due to dilution, transformation, and removal. Previous exposure
 692 of CDOM to solar radiation during transport from the head to the mouth of the Rhode River also plays a
 693 role in the decrease in CDOM photoreactivity along the estuarine gradient (Tzortziou et al., 2007). In
 694 addition to longer exposure time with transit along the salinity gradient, the water clarity at down-estuary
 695 sites is greater (Rose et al., 2018), allowing for greater exposure to sunlight (and thus lower
 696 photoreactivity) compared to more turbid waters closer to terrestrial margins. The greater photoreactivity
 697 of the Upper Muddy Creek (“non-marsh terrestrial”) compared to GCReW (“marsh”) is also likely
 698 impacted both by differences in CDOM source, as well as differences in previous UV-exposure. Canopy
 699 cover along the Upper Muddy Creek creates a more shaded environment compared to GCReW; this has
 700 been observed in other systems, such as streams, where an increase in canopy cover was associated with
 701 an increase in CDOM photoreactivity (Lu et al., 2013). In addition, water clarity in Muddy Creek is very
 702 low due to a high suspended matter concentration, which results in less CDOM exposure to sunlight (Rose
 703 et al., 2018). On the other hand, differences in turbidity between marsh tidal creeks did not explain the
 704 differences in photoreactivity that we observed across marsh sites (data not shown). Thus, any differences
 705 in photoreactivity between the marsh sites studied here was mostly driven by differences in DOM source.

706 The photoreactivity of marsh-exported CDOM showed small but statistically significant seasonal trends.
 707 There was an overall smaller relative change in $aCDOM300$, $S_{275-295}$, and S_R during the summer compared
 708 to the winter (Figures 7b-d). The observed seasonality in the change in $aCDOM300$, $S_{275-295}$, and S_R , and
 709 therefore, photobleaching, is likely driven both by the small differences in the relative contributions of
 710 various marsh-CDOM sources seasonally as well differences in UV-exposure prior to collection. Greater
 711 relative contributions of fresh marsh plant leachate in the summer, which has previously been shown to
 712 have a lower photoreactivity relative to soils (Chen & Jaffé, 2014), could partially explain why
 713 photoreactivity was lower in the summer relative to the winter, even if the contributions are small (C.D.
 714 Clark et al., 2008). Less prior exposure to UV-radiation in January, due to a lower sun angle, greater
 715 cloudiness, and shorter days, could also contribute to the greater CDOM photoreactivity in the winter
 716 compared to the summer. Previous studies in temperate streams and lakes showed that UV-radiation
 717 history was the main factor dictating photoreactivity for CDOM of similar source material (Cory et al.,
 718 2015; Lu et al., 2013 ; Osburn et al., 2001).

719 None of the initial optical properties predicted the observed spatiotemporal variability in CDOM
 720 photoreactivity, estimated as the change in S_R , except $S_{350-400}$ (Figure 9). The initial $S_{350-400}$ was the best
 721 predictor of photoreactivity for both the various sites within the Rhode River ($R^2 = 0.84, P < 0.01$) (Figure
 722 9a), across different marsh systems ($R^2 = 0.77, P < 0.01$) (Figure 9b), and both datasets combined ($R^2 =$

723 0.73, $P < 0.01$, data not shown). Other studies, based on water samples collected across a wide range of
 724 water types, have suggested that $S_{350-400}$ is a good proxy of CDOM molecular weight (Helms et al., 2008).
 725 Given that the change in $S_{350-400}$ by photobleaching is lower than the change in other absorption parameters
 726 such as $S_{275-295}$ (5-25% vs. 60-80%), $S_{350-400}$ could act as a proxy for the combined effects of both the
 727 original molecular weight of the source as well as previous UV exposure. While the history of
 728 photobleaching will impact the photoreactivity of CDOM, and these impacts are most easily observed in
 729 changes to $S_{275-295}$, we observed little variation in the change in $S_{275-295}$ across sites, even across sites with
 730 very different CDOM characteristics initially (Table 3, Figure 6b, and Figure 7d); however, the change in
 731 $S_{350-400}$ by photobleaching is directly related to differences in initial CDOM quality between sites (Table
 732 3, Figure 6b, and Figure 7e). As such, it could be argued that $S_{350-400}$ is better at predicting photoreactivity
 733 in both photobleached systems (Rhode River sites) as well as at sites with relatively un-altered CDOM
 734 (marsh and watershed sites), compared to other parameters that are more highly influenced by
 735 photobleaching. Interestingly, for predicting DOC loss for combined photobleaching and microbial
 736 degradation, $S_{350-400}$ was not a good predictor; instead, acDOM300 showed the best correlation out of all the
 737 measured optical parameters ($R^2 = 0.45$, $P < 0.01$, data not shown). While the combined photoreactivity
 738 and bioavailability of the winter CDOM was greater than the summer CDOM, both photobleaching and
 739 microbial degradation are likely more important CDOM removal processes in the summer due to higher
 740 levels of UV-radiation and higher summer water temperatures. UV-radiation exposure and temperature in
 741 our study were kept constant across samples despite these seasonal differences.



742

743 **Figure 9.** Initial $S_{350-400}$ as a predictor of combined photobleaching and microbial degradation, defined as
 744 the change in S_R over the 7-day light incubation, for (a) the Rhode River sites and (b) the marsh sites.

745 4.6 Jug Bay exports extremely bioavailable and photoreactive CDOM

746 Compared to other systems, the loss of both acDOM300 and DOC at Jug Bay over the 14-day microbial-
 747 only incubation was high, indicating particularly high bioavailability. Lu et al. (2013) reported DOC losses
 748 of 1-9% for 35-36 day incubations of stream DOM, under similar experimental conditions; Moran et al.,
 749 (2000) showed a DOC loss of 2.9% over their 51-day dark incubation. In our study, DOC from the Jug
 750 Bay system decreased on average by 11.7% over 14 days in the MD treatment, which is less than half the
 751 incubation time in Lu et al. (2013) and 3 times less than Moran et al., (2000). Moreover, for our microbial-
 752 only treatment, CDOM collected from Jug Bay showed only a small change in two of the humic-like
 753 components, C1 and C3, and a decrease in the longer-wavelength VIS- humic-like component, C2 (Figure
 754 5f-h), compared to the increases in C1, C2 and C3 observed in all other marsh sites. This could indicate
 755 either the lack of production of the humic-like components as seen in the other sites, or, the simultaneous
 756 microbial utilization and degradation of humic-like fluorescence, thus offsetting its production. Given that

757 Jug Bay also had a much higher loss in $a_{CDOM300}$ and DOC, a greater increase in S_R , and a greater decrease
758 in $S_{350-400}$ during the microbial-only incubations compared to the other sites, it is likely that the
759 microbially-produced, humic-like CDOM at Jug Bay is particularly bioavailable, and thus is being utilized
760 and degraded quickly.

761 The Jug Bay marsh system also exports highly photoreactive CDOM. The consistent loss of protein-like
762 CDOM fluorescence across all seasons at Jug Bay in the combined photobleaching and microbial
763 degradation treatment indicates that the protein-like CDOM at Jug Bay is more photoreactive than at the
764 other sites that showed a general increase in C4 (Figure 7i). In addition, Jug Bay had a significantly greater
765 increase in S_R and a greater loss in $S_{350-400}$ with light exposure than the other sites, further supporting
766 higher rates of photobleaching.

767 5 Conclusions

768 Through a complex interplay of physical and biological processes, marsh-estuary ecosystems are
769 important sources, reactors, and transformers of dissolved organic carbon and nutrients, regulating
770 biogeochemical exchanges along terrestrial-aquatic interfaces. Using a combination of field measurements
771 and laboratory incubations, our study captured the impact of photochemical and microbial processes on
772 marsh-exported CDOM across different seasons and systems characterized by different vegetation
773 properties, water quality, and salinity regimes. Photobleaching is mostly determined by the absorptivity,
774 molecular weight, and aromaticity of the CDOM, as well as previous exposure to UV-radiation; for our
775 samples, the potential for photobleaching was best estimated using $S_{350-400}$. In the summer, when
776 concentrated, high-molecular-weight, and aromatic marsh-exported CDOM received maximum exposure
777 to UV-radiation, photobleaching was an important process for CDOM transformation and, subsequently,
778 microbial degradation (J. B. Clark et al., 2019). CDOM photoreactivity decreased down-estuary away
779 from the marsh endmember, with increasing prior exposure and with a greater contribution of marine-
780 derived CDOM relative to terrestrially-derived CDOM. While marsh-export of CDOM and DOC showed
781 a strong seasonal cycle, with greater export in the summer, optical proxies for CDOM quality (e.g., S_R
782 and fluorescence PARAFAC ratios C2/C1, C3/C1, and C4/C1) showed considerably less seasonal and
783 interannual variability, suggesting the soil-buffering of marsh-DOM export. Marsh-exported CDOM
784 photoreactivity showed small but statistically significant seasonal dependence, with greater
785 photoreactivity measured on CDOM collected in the winter compared to the summer. Under natural
786 conditions, lower UV radiation in winter is expected to result in considerably less photochemical (and,
787 thus, also microbial) degradation of marsh-exported CDOM down-estuary. This suggests a greater relative
788 contribution of photoreactive, allochthonous CDOM down-estuary in the winter compared to the summer.

789 Because microbial degradation has been shown to both degrade absorbing and fluorescing CDOM and
790 produce fluorescing CDOM, the net effect of microbial processing on CDOM optical properties can vary
791 depending on the available substrate (Tranvik, 1988, 1993; Volk et al., 1997), nutrients, temperature
792 (Lønborg et al., 2009), bacterial communities (Kirchman et al., 2004; Logue et al., 2016), prior
793 photochemical degradation (this study; Reader & Miller, 2014), and other factors. In general, however,
794 we found that microbial degradation consistently resulted in a small increase in humic-like CDOM
795 fluorescence, and this increase is enhanced after exposure to light. Overall, microbial degradation offsets
796 the loss of humic-like CDOM fluorescence by photobleaching. Furthermore, microbial degradation within
797 the estuary is an autochthonous source of humic-like fluorescence typically associated with DOM of
798 terrigenous origin. Ultimately, the change in CDOM optical properties down-estuary is the combination
799 of microbial and photochemical degradation of terrigenous inputs, and autochthonous inputs of CDOM
800 that are also subject to microbial and photochemical processing.

801 Jug Bay is the most human-influenced site in terms of nutrient inputs and is also dominated by different
 802 (mostly non-persistent emergent) vegetation and soil characteristics than the other sites; as a result, it had
 803 both extremely photoreactive and bioavailable CDOM compared to the other marshes. The microbially-
 804 mediated loss of humic-like fluorescing CDOM at Jug Bay resulted in a smaller offset of photobleaching
 805 loss; therefore, this would likely result in lower concentrations of aromatic and high molecular weight
 806 CDOM persisting in the estuary. Because the protein-like CDOM fluorescence at Jug Bay is also
 807 photoreactive, this would also likely decrease with UV-exposure down-estuary. This has implications for
 808 how nutrient loading and eutrophic conditions in marsh-estuary systems might influence estuarine optical
 809 properties and biogeochemical cycling; a shift to more eutrophic marsh systems associated with more
 810 photo- and bio-labile CDOM could lead to higher rates of CDOM degradation and DOC loss in estuaries
 811 and, therefore, fewer inputs of refractory CDOM down-estuary and, ultimately, to marine environments.
 812 However, future work examining down-estuary trends seasonally across marshes of differing
 813 characteristics (e.g., eutrophic versus oligotrophic marsh-systems, marshes with differing vegetation) is
 814 needed.

815 In summary, our study has shown that CDOM source and UV exposure history play an important role in
 816 CDOM transformation processes, which vary seasonally, between marsh-systems, and down-estuary. We
 817 have shown that the 0.2 μm fraction should not be assumed to be sterile, since enough inoculum passes
 818 through the filter to result in significant microbial growth; this stresses the need for other methods of
 819 microbial growth inhibition that do not interfere with CDOM optics or photoreactivity in order to isolate
 820 the impacts of photobleaching alone. Few studies have examined the quality, bioavailability and
 821 photoreactivity of CDOM exported from marshes, and even fewer have compared marshes with varying
 822 characteristics and across seasons. Our study illustrates the role of photodegradation on bioavailability,
 823 and how these two processes interplay in marsh-estuarine systems to transform, degrade, and produce
 824 CDOM of differing qualities down-estuary. This would be particularly useful for comparison to
 825 biogeochemical model outputs to further constrain rates and fluxes in estuarine systems (J. B. Clark et al.,
 826 2019, 2020). Our results also have applications to remote sensing, which, in tandem with in situ
 827 measurements, can improve estimates of CDOM photoreactivity and bioavailability in coastal
 828 environments based on the characteristics of both the terrestrial and aquatic coastal landscape, such as
 829 land-use, marsh vegetation or soil, and in-water phytoplankton and sediment concentrations; this can be
 830 applied to help quantify carbon fluxes at scales much larger than a single marsh or sub-estuarine system.

831 Acknowledgements

832 This work was supported by the National Aeronautics and Space Administration (NASA) grant
 833 NNX14AP06G and the National Science Foundation (NSF) grant DEB-1556556, with additional support
 834 from NASA grant NNX14AM37G and NOAA Earth System Sciences and Remote Sensing Technologies
 835 award NA16SEC4810008. The authors would like to thank Dr. Patrick Megonigal, Andrew Peresta, and
 836 Jocelyn Mendez for their support during the field and laboratory measurements. The data used in this
 837 study are available in an online repository (<http://doi.org/10.5281/zenodo.4542308>).

838 References

839 Aulló-Maestro, M. E., Hunter, P., Spyros, E., Mercatoris, P., Kovács, A., Horváth, H., et al. (2016).
 840 Spatio-seasonal variability of chromophoric dissolved organic matter absorption and responses to
 841 photobleaching in a large shallow temperate lake. *Biogeosciences*, 14, 1215–1233.
 842 <https://doi.org/10.5194/bg-14-1215-2017>

843 Bianchi, T. S., Osburn, C. L., Shields, M. R., Yvon-Lewis, S., Young, J., Guo, L., & Zhou, Z. (2014).
 844 Deepwater horizon oil in Gulf of Mexico waters after 2 years: Transformation into the dissolved

845 organic matter pool. *Environmental Science and Technology*, 48(16), 9288–9297.
 846 <https://doi.org/10.1021/es501547b>

847 Brailsford, F. L., Glanville, H. C., Marshall, M. R., Golyshin, P. N., Johnes, P. J., Yates, C. A., et al.
 848 (2017). Microbial use of low molecular weight DOM in filtered and unfiltered freshwater: Role of
 849 ultra-small microorganisms and implications for water quality monitoring. *Science of the Total
 850 Environment*, 598, 377–384. <https://doi.org/10.1016/j.scitotenv.2017.04.049>

851 Bricaud, A., Morel, A., & Prieur, L. (1981). Absorption by dissolved organic matter to the sea (Yellow
 852 substance) in the UV and visible domains. *Limnology and Oceanography*, 26(1), 43–53.

853 Chen, M., & Jaffé, R. (2014). Photo- and bio-reactivity patterns of dissolved organic matter from biomass
 854 and soil leachates and surface waters in a subtropical wetland. *Water Research*, 61, 181–190.
 855 <https://doi.org/10.1016/j.watres.2014.03.075>

856 Clark, C. D., Litz, L. P., & Grant, S. B. (2008). Salt marshes as a source of chromophoric dissolved organic
 857 matter (CDOM) to Southern California coastal waters. *Limnology and Oceanography*, 53(5), 1923–
 858 1933. <https://doi.org/10.4319/lo.2008.53.5.1923>

859 Clark, J. B., Neale, P. J., Tzortziou, M., Cao, F., & Hood, R. R. (2019). A mechanistic model of
 860 photochemical transformation and degradation of colored dissolved organic matter. *Marine
 861 Chemistry*, 214. <https://doi.org/10.1016/j.marchem.2019.103666>

862 Clark, J. B., Long, W., & Hood, R. R. (2020). A Comprehensive Estuarine Dissolved Organic Carbon
 863 Budget Using an Enhanced Biogeochemical Model. *Journal of Geophysical Research: Biogeosciences*, 125(5), 1–21. <https://doi.org/10.1029/2019JG005442>

865 Coble, P. G. (1996). Characterization of marine and terrestrial DOM in seawater using excitation emission
 866 matrix spectroscopy. *Marine Chemistry*, 51, 325–346. [https://doi.org/10.1016/0304-4203\(95\)00062-3](https://doi.org/10.1016/0304-4203(95)00062-3)

868 Cory, R. M., Harrold, K. H., Neilson, B. T., & Kling, G. W. (2015). Controls on dissolved organic matter
 869 (DOM) degradation in a headwater stream: The influence of photochemical and hydrological
 870 conditions in determining light-limitation or substrate-limitation of photo-degradation.
 871 *Biogeosciences*, 12, 6669–6685. <https://doi.org/10.5194/bg-12-6669-2015>

872 Dai, M., Yin, Z., Meng, F., Liu, Q., & Cai, W. (2012). Spatial distribution of riverine DOC inputs to the
 873 ocean: an updated global synthesis. *Current Opinion in Environmental Sustainability*, 4, 170–178.
 874 <https://doi.org/10.1016/j.cosust.2012.03.003>

875 Dalzell, B. J., Minor, E. C., & Mopper, K. (2009). Photodegradation of estuarine dissolved organic matter:
 876 a multi-method assessment of DOM transformation. *Organic Geochemistry*, 40, 243–257.
 877 <https://doi.org/10.1016/j.orggeochem.2008.10.003>

878 DuPont. (2011). *DuPont Fluoropolymers*.

879 Elhadidy, A. M., van Dyke, M. I., Peldszus, S., & Huck, P. M. (2016). Application of flow cytometry to
 880 monitor assimilable organic carbon (AOC) and microbial community changes in water. *Journal of
 881 Microbiological Methods*, 130, 154–163. <https://doi.org/10.1016/j.mimet.2016.09.009>

882 Fellman, J. B., Amore, D. V. D., Hood, E., & Boone, R. D. (2008). Fluorescence characteristics and
 883 biodegradability of dissolved organic matter in forest and wetland soils from coastal temperate
 884 watersheds in southeast Alaska. *Biogeochemistry*. <https://doi.org/10.1007/s10533-008-9203-x>

885 Fellman, J. B., Hood, E., & Spencer, R. G. M. (2010). Fluorescence spectroscopy opens new windows
886 into dissolved organic matter dynamics in freshwater ecosystems: A review. *Limnology and*
887 *Oceanography*, 55(6), 2452–2462. <https://doi.org/10.4319/lo.2010.55.6.2452>

888 Fellman, J. B., Petrone, K. C., & Grierson, P. F. (2011). Source, biogeochemical cycling, and fluorescence
889 characteristics of dissolved organic matter in an agro-urban estuary. *Limnology and Oceanography*,
890 56(1), 243–256. <https://doi.org/10.4319/lo.2011.56.1.0243>

891 Fritz, J. J., Neale, P. J., Davis, R. F., & Peloquin, J. A. (2008). Response of Antarctic phytoplankton to
892 solar UVR exposure: Inhibition and recovery of photosynthesis in coastal and pelagic assemblages.
893 *Marine Ecology Progress Series*, 365, 1–16.

894 Guo, W., Xu, J., Wang, J., Wen, Y., Zhuo, J., & Yan, Y. (2010). Emission Matrix Fluorescence
895 Spectroscopy and Parallel Factor Analysis Je Sc Sc. *Journal of Environmental Sciences*, 22(11),
896 1728–1734.

897 Hansell, D., Carlson, C. A., Repeta, D., & Schlitzer, R. (2009). Dissolved Organic Matter in the Ocean:
898 A Controversy Stimulates New Insights. *Oceanography*, 22, 202–211.
899 <https://doi.org/10.5670/oceanog.2009.109>

900 Hedges, J. I. (1992). Global biogeochemical cycles: progress and problems. *Marine Chemistry*, 39, 67–
901 93.

902 Helms, J. R., Stubbins, A., Ritchie, J. D., Minor, E. C., Kieber, D. J., & Mopper, K. (2008). Absorption
903 spectral slopes and slope ratios as indicators of molecular weight, source, and photobleaching of
904 chromophoric dissolved organic matter. *Limnology and Oceanography*, 53(3), 955–969.
905 <https://doi.org/10.4319/lo.2008.53.3.0955>

906 Henry, B. J., Carlin, J. P., Hammerschmidt, J. A., Buck, R. C., Buxton, L. W., Fiedler, H., et al. (2018).
907 A critical review of the application of polymer of low concern and regulatory criteria to
908 fluoropolymers. *Integrated Environmental Assessment and Management*, 14(3), 316–334.
909 <https://doi.org/10.1002/ieam.4035>

910 Hernes, P. J. (2003). Photochemical and microbial degradation of dissolved lignin phenols: Implications
911 for the fate of terrigenous dissolved organic matter in marine environments. *Journal of Geophysical*
912 *Research*, 108(C9), 3291. <https://doi.org/10.1029/2002JC001421>

913 Jordan, T. E., Correll, D. L., & Whigham, D. F. (1983). Nutrient Flux in the Rhode River - Tidal Exchange
914 of Nutrients by Brackish Marshes. *Estuarine, Coastal and Shelf Science*, 17, 651–667.

915 Jordan, T. E., Correll, D. L., Miklas, J., & Weller, D. E. (1991a). Long-term trends in estuarine nutrients
916 and chlorophyll, and short- term effects of variation in watershed discharge. *Marine Ecology*
917 *Progress Series*, 75(2–3), 121–132. <https://doi.org/10.3354/meps075121>

918 Jordan, T. E., Correll, D. L., Miklas, J., & Weller, D. E. (1991b). Nutrients and chlorophyll at the interface
919 of a watershed and an estuary. *Limnology and Oceanography*, 36(2), 251–267.

920 Kahle, D., & Wickham, H. (2013). ggmap: Spatial Visualization with ggplot2. *The R Journal*, 5(1), 144–
921 161.

922 Karth, R., Domotor, D., Golden, R., Karrh, L., Landry, B., Romano, W., et al. (2013). *Patuxent River*
923 *Water Quality and Habitat Assessment*.

924 Kirchman, D. L., Dittel, A. I., Findlay, S. E. G., & Fischer, D. T. (2004). Changes in bacterial activity and

925 community structure in response to dissolved organic matter in the Hudson River, New York. *Aquatic*
 926 *Microbial Ecology*, 35, 243–257. <https://doi.org/10.3354/ame035243>

927 Kothawala, D. N., Murphy, K. R., Stedmon, C. A., Weyhenmeyer, G. A., & Tranvik, L. J. (2013). Inner
 928 filter correction of dissolved organic matter fluorescence. *Limnology and Oceanography: Methods*,
 929 11(DEC), 616–630. <https://doi.org/10.4319/lom.2013.11.616>

930 Lee, S., Kang, Y. C., & Fuhrman, J. A. (1995). Imperfect retention of natural bacterioplankton cells by
 931 glass fiber filters. *Marine Ecology Progress Series*, 119, 285–290.
 932 <https://doi.org/10.3354/meps119285>

933 Liu, J., Li, B., Wang, Y., Zhang, G., Jiang, X., & Li, X. (2019). Passage and community changes of
 934 filterable bacteria during microfiltration of a surface water supply. *Environment International*,
 935 131(March), 104998. <https://doi.org/10.1016/j.envint.2019.104998>

936 Logue, J. B., Stedmon, C. A., Kellerman, A. M., Nielsen, N. J., Andersson, A. F., Laudon, H., et al. (2016).
 937 Experimental insights into the importance of aquatic bacterial community composition to the
 938 degradation of dissolved organic matter. *The ISME Journal*, 10, 533–545.
 939 <https://doi.org/10.1038/ismej.2015.131>

940 Lønborg, C., Davidson, K., Álvarez-Salgado, X. A., & Miller, A. E. J. (2009). Bioavailability and bacterial
 941 degradation rates of dissolved organic matter in a temperate coastal area during an annual cycle.
 942 *Marine Chemistry*, 113, 219–226. <https://doi.org/10.1016/j.marchem.2009.02.003>

943 Lu, Y., Bauer, J. E., Canuel, E. A., Yamashita, Y., Chambers, R. M., & Jaffé, R. (2013). Photochemical
 944 and microbial alteration of dissolved organic matter in temperate headwater streams associated with
 945 different land use. *Journal of Geophysical Research: Biogeosciences*, 118, 566–580.
 946 <https://doi.org/10.1002/jgrg.20048>

947 Luef, B., Frischkorn, K. R., Wrighton, K. C., Holman, H. Y. N., Birarda, G., Thomas, B. C., et al. (2015).
 948 Diverse uncultivated ultra-small bacterial cells in groundwater. *Nature Communications*, 6.
 949 <https://doi.org/10.1038/ncomms7372>

950 MacDonell, M. T., & Hood, M. A. (1982). Isolation and characterization of ultramicrobacteria from a gulf
 951 coast estuary. *Applied and Environmental Microbiology*, 43(3), 566–571.
 952 <https://doi.org/10.1128/aem.43.3.566-571.1982>

953 Maie, N., Scully, N. M., Pisani, O., & Jaffé, R. (2007). Composition of a protein-like fluorophore of
 954 dissolved organic matter in coastal wetland and estuarine ecosystems. *Water Research*, 41, 563–570.
 955 <https://doi.org/10.1016/j.watres.2006.11.006>

956 Medeiros, P. M., Seidel, M., Gifford, S. M., Ballantyne, F., Dittmar, T., Whitman, W. B., & Moran, M.
 957 A. (2017). Microbially-mediated transformations of estuarine dissolved organic matter. *Frontiers in*
 958 *Marine Science*, 4. <https://doi.org/10.3389/fmars.2017.00069>

959 Meybeck, M. (1982). Carbon, nitrogen, and phosphorous transport by world rivers. *Science*, 282, 401–
 960 450.

961 Miller, W. L., & Moran, M. A. (1997). Interaction of photochemical and microbial processes in the
 962 degradation of refractory dissolved organic matter from a coastal marine environment. *Limnology*
 963 *and Oceanography*, 42, 1317–1324. <https://doi.org/10.4319/lo.1997.42.6.1317>

964 Moran, M. A., Sheldon, W. M., & Sheldon, J. E. (1999). Biodegradation of riverine dissolved organic
 965 carbon in five estuaries of the southeastern United States. *Estuaries*, 22(1), 55–64.

966 <https://doi.org/10.2307/1352927>

967 Moran, M. A., Sheldon Jr., W. M., & Zepp, R. G. (2000). Carbon loss and optical property changes during
968 long-term photochemical and biological degradation of estuarine dissolved organic matter.
969 *Limnology and Oceanography*, 45(6), 1254–1264. <https://doi.org/10.4319/lo.2000.45.6.1254>

970 Murphy, K. R., Hambly, A., Singh, S., Henderson, R. K., Baker, A., Stuetz, R., & Khan, S. J. (2011).
971 Organic matter fluorescence in municipal water recycling schemes: Toward a unified PARAFAC
972 model. *Environmental Science and Technology*, 45(7), 2909–2916.
973 <https://doi.org/10.1021/es103015e>

974 Murphy, K. R., Stedmon, C. A., Wenig, P., & Bro, R. (2014). OpenFluor- an online spectral library of
975 auto-fluorescence by organic compounds in the environment. *Analytical Methods*, 6(3), 658–661.
976 <https://doi.org/10.1039/C3AY41935E>

977 Neale, P. J., & Fritz, J. J. (2002). Experimental exposure of plankton suspensions to polychromatic
978 ultraviolet radiation for determination of spectral weighting functions. *Ultraviolet Ground- and*
979 *Space-Based Measurements, Models, and Effects*, 4482, 291–296. <https://doi.org/10.1117/12.452930>

980 Nelson, N. B., Carlson, C. A., & Steinberg, D. K. (2004). Production of chromophoric dissolved organic
981 matter by Sargasso Sea microbes. *Marine Chemistry*, 89, 273–287.
982 <https://doi.org/10.1016/j.marchem.2004.02.017>

983 Nixon, S. W. (1980). Between coastal marshes and coastal waters - a review of twenty years of speculation
984 and research on the role of salt marshes in estuarine productivity and water chemistry. In P. Hamilton
985 & K. B. Macdonald (Eds.), *Estuarine and Wetland Processes* (pp. 438–525).
986 https://doi.org/https://doi.org/10.1007/978-1-4757-5177-2_20

987 Obayashi, Y., & Suzuki, S. (2019). High growth potential of transiently 0.2-μm-filterable bacteria with
988 extracellular protease activity in coastal seawater. *Plankton and Benthos Research*, 14(4), 276–286.
989 <https://doi.org/10.3800/pbr.14.276>

990 Osburn, C. L., & Stedmon, C. A. (2011). Linking the chemical and optical properties of dissolved organic
991 matter in the Baltic-North Sea transition zone to differentiate three allochthonous inputs. *Marine*
992 *Chemistry*, 126(1–4), 281–294. <https://doi.org/10.1016/j.marchem.2011.06.007>

993 Osburn, C. L., Zagarese, H. E., Morris, D. P., Hargreaves, B. R., & Cravero, W. E. (2001). Calculation of
994 spectral weighting functions for the solar photobleaching of chromophoric dissolved organic matter
995 in temperate lakes. *Limnology and Oceanography*, 46. <https://doi.org/10.4319/lo.2001.46.6.1455>

996 Osburn, C. L., Handsel, L. T., Mikan, M. P., Paerl, H. W., & Montgomery, M. T. (2012). Fluorescence
997 tracking of dissolved and particulate organic matter quality in a river-dominated estuary.
998 *Environmental Science and Technology*, 46(16), 8628–8636. <https://doi.org/10.1021/es3007723>

999 Osburn, C. L., Mikan, M. P., Etheridge, J. R., Burchell, M. R., & Birgand, F. (2015). Seasonal variation
1000 in the quality of dissolved and particulate organic matter exchanged between a salt marsh and its
1001 adjacent estuary. *Journal of Geophysical Research: Biogeosciences*, 120, 1430–1449.
1002 <https://doi.org/10.1002/2014JG002897>

1003 Osburn, C. L., Boyd, T. J., Montgomery, M. T., Bianchi, T. S., Coffin, R. B., & Paerl, H. W. (2016).
1004 Optical proxies for terrestrial dissolved organic matter in estuaries and coastal waters. *Frontiers in*
1005 *Marine Science*, 2(JAN). <https://doi.org/10.3389/fmars.2015.00127>

1006 Osburn, C. L., Handsel, L. T., Peierls, B. L., & Paerl, H. W. (2016). Predicting Sources of Dissolved

1007 Organic Nitrogen to an Estuary from an Agro-Urban Coastal Watershed. *Environmental Science and*
 1008 *Technology*, 50(16), 8473–8484. <https://doi.org/10.1021/acs.est.6b00053>

1009 Perry, J. E., & Atkinson, R. B. (1997). Plant Diversity Along a Salinity Gradient of Four Marshes on the
 1010 York and Pamunkey Rivers in Virginia. *Castanea*, 62(2), 112–118.

1011 Pinsonneault, A. J., Megonigal, J. P., Neale, P. J., Tzortziou, M., Canuel, E. A., Pondell, C. R., et al.
 1012 (2020). Dissolved Organic Carbon Sorption Dynamics in Tidal Marsh Soils. *Limnology and*
 1013 *Oceanography, in Review*.

1014 Ruggaber, A., Dlugi, R., & Nakajima, T. (1994). Modeling of radiation quantities and photolysis
 1015 frequencies in the troposphere. *Journal of Atmospheric Chemistry*, 18, 171–210.

1016 Putter, A. (1907). Der Stoffhaushalt des Meeres. *Allgemeine Physiologie*, 7, 321–368.

1017 Qualls, R. G., Haines, B. L., & Swank, W. T. (1991). Fluxes of Dissolved Organic Nutrients and Humic
 1018 Substances in a Deciduous Forest. *Ecology*, 72(1), 254–266.

1019 Reader, H. E., & Miller, W. L. (2014). The efficiency and spectral photon dose dependence of
 1020 photochemically induced changes to the bioavailability of dissolved organic carbon. *Limnology and*
 1021 *Oceanography*, 59(1), 182–194. <https://doi.org/10.4319/lo.2014.59.1.0182>

1022 Retelletti Brogi, S., Derrien, M., & Hur, J. (2019). In-Depth Assessment of the Effect of Sodium Azide
 1023 on the Optical Properties of Dissolved Organic Matter. *Journal of Fluorescence*, 29(4), 877–885.
 1024 <https://doi.org/10.1007/s10895-019-02398-w>

1025 Rochelle-Newall, E. J., & Fisher, T. R. (2002). Production of chromophoric dissolved organic matter
 1026 fluorescence in marine and estuarine environments: An investigation into the role of phytoplankton.
 1027 *Marine Chemistry*, 77, 7–21. [https://doi.org/10.1016/S0304-4203\(01\)00072-X](https://doi.org/10.1016/S0304-4203(01)00072-X)

1028 Rose, K. C., Neale, P. J., Tzortziou, M., Gallegos, C. L., & Jordan, T. E. (2018). Patterns of spectral,
 1029 spatial, and long-term variability in light attenuation in an optically complex sub-estuary. *Limnology*
 1030 *and Oceanography*, 64, 257–272. <https://doi.org/10.1002/lno.11005>

1031 Santos, L., Santos, E. B. H., Dias, J. M., Cunha, Â., & Almeida, A. (2014). Photochemical and microbial
 1032 alterations of DOM spectroscopic properties in the estuarine system Ria de Aveiro. *Photochemical*
 1033 *and Photobiological Sciences*, 13, 1146–1159. <https://doi.org/10.1039/C4PP00005F>

1034 Schlesinger, W. H., & Bernhardt, E. S. (2013). *Biogeochemistry: An analysis of global change* (3rd ed.).
 1035 Waltham, MA and Oxford, UK: Elsevier, Inc.

1036 Seitzinger, S. P., Harrison, J. A., & Dumont, E. (2005). Sources and delivery of carbon, nitrogen, and
 1037 phosphorus to the coastal zone: An overview of Global Nutrient Export from Watersheds (NEWS)
 1038 models and their application. *Global Biogeochemical Cycles*, 19, 1–11.
 1039 <https://doi.org/10.1029/2005GB002606>

1040 Shultz, M., Pellerin, B., Aiken, G. R., Martin, J., & Raymond, P. A. (2018). High Frequency Data Exposes
 1041 Nonlinear Seasonal Controls on Dissolved Organic Matter in a Large Watershed. *Environmental*
 1042 *Science and Technology*, 52, 5644–5652.

1043 Stedmon, C. A., & Bro, R. (2008). Characterizing dissolved organic matter fluorescence with parallel
 1044 factor analysis: a tutorial. *Limnology and Oceanography: Methods*, 6, 572–579.
 1045 <https://doi.org/10.4319/lom.2008.6.572>

1046 Stedmon, C. A., & Markager, S. (2005). Tracing the production and degradation of autochthonous

1047 fractions of dissolved organic matter using fluorescence analysis. *Limnology and Oceanography*,
 1048 50(5), 1415–1426. <https://doi.org/10.4319/lo.2005.50.5.1415>

1049 Swarth, C. W., Delgado, P., & Whigham, D. F. (2013). Vegetation Dynamics in a Tidal Freshwater
 1050 Wetland: A Long-Term Study at Differing Scales. *Estuaries and Coasts*, 36, 559–574.
 1051 <https://doi.org/10.1007/s12237-012-9568-x>

1052 Tanaka, K., Kuma, K., Hamasaki, K., & Yamashita, Y. (2014). Accumulation of humic-like fluorescent
 1053 dissolved organic matter in the Japan Sea. *Scientific Reports*, 4, 1–7.
 1054 <https://doi.org/10.1038/srep05292>

1055 Thurman, E. M. (1985). *Organic geochemistry of natural waters*. Dordrecht, The Netherlands: Martinus
 1056 Nijhoff/Dr W. Junk Publishers.

1057 Tranvik, L. J. (1988). Availability of Dissolved Organic Carbon for Planktonic Bacteria in Oligotrophic
 1058 Lakes of Differing Humic Content. *Microbial Ecology*, 16, 311–322.

1059 Tranvik, L. J. (1993). Microbial transformation of labile dissolved organic matter into humic-like matter
 1060 in seawater. *FEMS Microbiology Ecology*, 12, 177–183. [https://doi.org/10.1016/0168-6496\(93\)90013-W](https://doi.org/10.1016/0168-6496(93)90013-W)

1062 Tranvik, L. J., Olofsson, H., & Bertilsson, S. (1999). Photochemical effects on bacterial degradation of
 1063 dissolved organic matter in lake water. *Microbial Biosystems: New Frontiers*.

1064 Tzortziou, M., Osburn, C. L., & Neale, P. J. (2007). Photobleaching of dissolved organic material from a
 1065 tidal marsh-estuarine system of the Chesapeake Bay. *Photochemistry and Photobiology*, 83, 782–
 1066 792. <https://doi.org/10.1111/j.1751-1097.2007.00142.x>

1067 Tzortziou, M., Neale, P. J., Osburn, C. L., Megonigal, J. P., Maie, N., & Jaffé, R. (2008). Tidal marshes
 1068 as a source of optically and chemically distinctive colored dissolved organic matter in the Chesapeake
 1069 Bay. *Limnology and Oceanography*, 53(1), 148–159. <https://doi.org/10.4319/lo.2008.53.1.0148>

1070 Tzortziou, M., Neale, P. J., Megonigal, J. P., Lee Pow, C., & Butterworth, M. (2011). Spatial gradients in
 1071 dissolved carbon due to tidal marsh outwelling into a Chesapeake Bay estuary. *Marine Ecology
 1072 Progress Series*, 426, 41–56. <https://doi.org/10.3354/meps09017>

1073 Volk, C. J., Volk, C. B., & Kaplan, L. A. (1997). Chemical composition of biodegradable dissolved
 1074 organic matter in streamwater. *Limnology and Oceanography*, 42(1), 39–44.
 1075 <https://doi.org/10.4319/lo.1997.42.1.0039>

1076 Wagner, S., Jaffé, R., Cawley, K., Dittmar, T., & Stubbins, A. (2015). Associations Between the Molecular
 1077 and Optical Properties of Dissolved Organic Matter in the Florida Everglades, a Model Coastal
 1078 Wetland System. *Frontiers in Chemistry*, 3. <https://doi.org/10.3389/fchem.2015.00066>

1079 Wang, Y., Hammes, F., Boon, N., & Egli, T. (2007). Quantification of the filterability of freshwater
 1080 bacteria through 0.45, 0.22, and 0.1 μm pore size filters and shape-dependent enrichment of filterable
 1081 bacterial communities. *Environmental Science and Technology*, 41(20), 7080–7086.
 1082 <https://doi.org/10.1021/es0707198>

1083 Wang, Y., Hammes, F., Düggelin, M., & Egli, T. (2008). Influence of size, shape, and flexibility on
 1084 bacterial passage through micropore membrane filters. *Environmental Science and Technology*,
 1085 42(17), 6749–6754. <https://doi.org/10.1021/es800720n>

1086 Ward, N. D., Megonigal, J. P., Bond-Lamberty, B., Bailey, V. L., Butman, D., Canuel, E. A., et al. (2020).

1087 Representing the function and sensitivity of coastal interfaces in Earth system models. *Nature*
1088 *Communications*, 11(1), 1–14. <https://doi.org/10.1038/s41467-020-16236-2>

1089 Wetzel, R. G. (1992). Gradient-dominated ecosystems: sources and regulatory functions of dissolved
1090 organic matter in freshwater ecosystems. *Hydrobiologia*, 181–198.

1091 Windham-Myers, L., Cai, W.-J., Alin, S. R., Andersson, A., Crosswell, J., Herrmann, J. M., et al. (2018).
1092 *Chapter 15: Tidal wetlands and estuaries*. (N. Cavallaro, G. Shrestha, R. Birdsey, M. A. Mayes, R.
1093 G. Najjar, S. C. Reed, et al., Eds.), *Second State of the Carbon Cycle Report (SOCCR2): A Sustained*
1094 *Assessment Report*. Washington, DC, USA. Retrieved from
1095 <https://doi.org/10.7930/SOCCR2.2018.Ch15>.

1096 Yamashita, Y., Jaffé, R., Maie, N., & Tanoue, E. (2008). Assessing the dynamics of dissolved organic
1097 matter (DOM) in coastal environments by excitation emission matrix fluorescence and parallel factor
1098 analysis (EEM-PARAFAC). *Limnology and Oceanography*, 53(5), 1900–1908.
1099 <https://doi.org/10.4319/lo.2008.53.5.1900>

1100 Yamashita, Y., Scinto, L. J., Maie, N., & Jaffé, R. (2010). Dissolved Organic Matter Characteristics
1101 Across a Subtropical Wetland's Landscape: Application of Optical Properties in the Assessment of
1102 Environmental Dynamics. *Ecosystems*, 13, 1006–1019. <https://doi.org/10.1007/s10021-010-9370-1>

1103 Zhang, Y., Liu, X., Osburn, C. L., Wang, M., Qin, B., & Zhou, Y. (2013). Photobleaching Response of
1104 Different Sources of Chromophoric Dissolved Organic Matter Exposed to Natural Solar Radiation
1105 Using Absorption and Excitation-Emission Matrix Spectra. *PLoS ONE*, 8(10).
1106 <https://doi.org/10.1371/journal.pone.0077515>